Observations by the Editor

Obs. 1:

Methods: The methods are not always clearly described. In particular, in section 3.3, the Fourier transform procedure does not make sense. The IFFT is usually used to convert from the frequency domain to the space domain, not the other way around. The expression "The signal obtained from each step of the FFT decomposition" does not mean anything to me, and the statement that "By studying the progression of these variations, the frequency of the second mode showed the highest frequency where the Sdev reaches an equilibrium" needs to be rewritten, as it does not correspond to anything I understand about signal processing.

Response:

Sections 3 and 4 were rewritten and reformulated accordingly and the focus of the analysis was modified. With these changes we aim to emphasize that the analysis using FFT aimed to extract low frequency oscillations from a noisy signal obtained from the isotope record. The filtered signal was then compared with meteorological data retrieved from re-analysis data using a linear regression analysis. The linear regression model was fitted to the whole data set and in this way the signal was transformed from the space domain (depth) to the time domain (age). Thereafter temperature, accumulation rate and environmental conditions trends were reconstructed.

Obs. 2:

I think what is going on is that the authors looked at the FFT spectrum of the signal and decided what parts of it were meaningful, then edited out the higher-frequency, less meaningful portion and used the IFFT to produce a filtered signal containing only low-frequency information. They then matched the peaks and troughs of the two d signal to date the core. What is not clear is whether only a single rescaling value was adequate to match the core and the meterological signal, or whether different stretching values were used to move each peak in the core inline with the meterological signal. I, and the referees, assumed the latter, based on which the correlations drawn between the core and the meterological signal are meaningless. Under this understanding, the authors' explanation that the correlation was between the composite core and the meterological records is not helpful, because the composite core would suffer the same, or nearly the same, spurious correlation with the meterological data. If only a single stretching value was used, then the correlations between the two signals may be significant. Someone familiar with standard English terminology for Fourier analysis needs to read and revise this section carefully.

Response:

This section has been rewritten to make it clear that the stretching value we found via the comparison with the modeled d-excess has been applied to the complete dataset, we have not stretched specific sections with different values. The correlations can therefore be calculated using the standard method and the number of degrees of freedom is n-2. All alpha values are 0.05 and we have therefore removed them from the text. Instead we indicate the degrees of freedom (n-2) for all correlations.

Obs. 3:

Results: As in previous versions, the motivation for the correlations presented in section 4 were not at all easy to follow in the revised manuscript. Each time the authors compare two variables and calculate a correlation value between them, the need to explain WHY they performed this correlation, WHAT they expected to learn from the correlation, and what the statistical test indicates.

Response:

Section 4 has been carefully reviewed and rewritten in order to make the objective of each analysis clear. This new version explicitly states for each comparison, what is the specific aim and result obtained from each analysis.

Obs. 4:

The alpha values now included in the manuscript do not generally add clarity to the results: much more helpful would be to list the number of degrees of freedom in the correlations that was used in calculating the p values. Presenting the correlation results in line with the text generally makes the paper much harder to read. In particular, the long paragraph in 4.1.1 could be improved by presenting the s values and their significance statistics in a separate table, along with the monthly correlations.

Response:

As explained in the response to Obs. 2, we thoroughly revised and reformulated Section 4. The number of degrees of freedom were added to each calculation. All slope, significance level, standard errors and further statistical data is presented in Table 4 and only strictly necessary information is shown in the text.

Obs. 5:

Section 4.1.1, line 25: This sentence: "Thus, the time series of monthly averages shows a positive correlation between both parameters" did not seem to follow from the other material in the paragraph, which is largely about the daily correlations (the s values).

Response:

This sentence has been removed. This sentence was no longer needed, and unfortunately we failed to eliminate it in the last version.

Obs. 6:

General considerations: The use of the terms "inverse/direct behavior" and "inverse/direct relationship" remains common in the manuscript. I recommended, and the reviewers agreed, that this expression should not be used, and that "positive/negative correlation" should be used instead.

Response:

We regret that we didn´t correct this properly. We have now reviewed this terminology to only use positive/negative correlation.

Obs. 7:

The authors need to break the discussion section into shorter paragraphs, with a topic sentence for each to indicate what point they are trying to make, and why. The very long paragraphs used here are difficult to untangle, and the line of the argument gets lost.

Response:

The entire paper has been reworked to improve its structure, coherence and to better direct the reader towards an improved understanding of our results and discussion. We firmly believe that this was achieved in this updated version.

Non-public comments to the Author:

Dear Dr. Fernandoy, After the second round of revisions, a manuscript like this should be very close to ready for publication. I do not see that this is the case here. I think the referees have made a good effort at reviewing the manuscript again, but do not have the patience to provide detailed comments on the results and discussion sections of the paper, except to echo some of the points that I have made about them. Before I would be willing to send a revised manuscript out for more reviews, I would like to see extensive revisions to the results and discussion sections so that the reader can easily follow why each step in the correlation analysis was performed, and what the results mean. I would also like to see extensive editing for English, following my recommendations against the use of the terms 'direct/inverse relationship.' I also would like to see an acknowledgement of the potential for spurious correlation between the stretched meterological record and the core, and a good justification for why the correlation is potentially significant (if it is.). While this may seem a minor point, it is something that will be important to anyone interested in trying the same method for their own core.

Response:

Dear Dr. Smith, Firstly on behalf of the co-authors, I would like to apologize for the frustration caused whilst editing this manuscript. In review of the publication, we realized that the methods needed to be rewritten to put the results and discussion sections into context. Subsequent to clarifying the methods used, we rewrote sections of the results and discussion to clarify the outcomes and related interpretations. For this purpose, we invited two new co-authors with extensive scientific and publishing experience. Dr. Shelley MacDonell is widely re-known glaciologist and hydrologist, adding that she is a native English Speaker. Dr. Fabrice Lambert is a statistics and glacio-chemistry expert. Both have been directly involved in editing the whole manuscript, adding a deeper insight into the statistical treatment and improving the scientific integrity of the manuscript, as well as improving language and terminology issues found in the previous versions. Within this process, we focused on using a more direct approach, which is related to extensive English editing. We hope that the new version clarifies the approach we have taken and that within the new version, the impact of our results will be more apparent. We appreciate the time that you and the reviewers have taken in revising this manuscript, and regret the time it has taken to improve the manuscript, hopefully to the point of now being publishable.

Observations by Reviewer 1

Comments on New regional insights into the stable water isotope signal at the northern Antarctic Peninsula as tools for climate studies, Fernandoy et al. The manuscript presents valuable glacio-chemical data for the northern area of the Antarctic Peninsula. The authors present water stable isotope data sets of precipitation and firn cores collected near O'Higgins station. The authors use an innovative method to obtain the time scale of the firn cores which, the authors claim, cannot be dated by traditional methods such as annual cycles counting in the d18O profile. The authors then discuss the isotope-temperature relationship at different seasons and conclude that an isotope-temperature relationship cannot be valid for all seasons, but rather depends on seasonal variability of oceanic conditions. This is the second time revising this manuscript. Many of the comments in the first revision have been addressed and the manuscript has improved accordingly. However, I still find relevant points that were not addressed by the authors in the final corrected version of the manuscript. These should be addressed before the paper is considered for publication.

Response:

Firstly, we regret overlooking comments made on the previous version of this paper. In this iteration, we have carefully considered each of the reviewer's comments, and have edited the document as appropriate. We would like to thank the reviewer for their detailed review of this publication.

General comments

Obs. 1:

In section 3.1, please indicate how the precipitation samples were collected, type of sample collector, sample bottles, handling and storage, etc.

Response:

This information has been included in Section 3.1.

Obs. 2:

RC. In section 3.2: please indicate the basis to the -1.4C latitudinal correction. It is not clear for me how the authors got the -1.4 C factor, this should be clear in the manuscript. The authors added a figure in the first response letter, but it is still not clear to me how they obtained the -1.4 factor.

Response:

This correction is based on the difference of mean temperature between the two automatic weather stations (Bellingshausen and O´Higgins). They have a high correlation (R = 0.97), and show similar temperature oscillations at a daily scale. O´Higgins Station is on average 1.4°C colder than Bellingshausen Station, and is located around 150 km south of Bellingshausen. Therefore, this latitudinal difference is what we originally referred to as the "latitude correction". Due to the confusion in the name, we have changed it to be "temperature correction". We added the following explication to the text: "The temperature record from OH contains several large data gaps, and so the available data from 1968 to 2015 were compared with those measured at BE to evaluate the possibility of lapsing data from BE to the site due to the data continuity available (uninterrupted record since 1968). The BE and OH data are highly correlated (R=0.97, p<0.01), and so a correction of -1.4ºC was applied to the BE data based on linear regression analysis."

Obs. 3:

When calculating the R values, the authors indicate alpha, however, they do not indicate if the R values were corrected considering the degrees of freedom of the system. That should be included.

Response:

See response to observation 2 from the Editor. To summarize: the stretching value estimated from the comparison with modeled d-excess has been applied to the complete dataset, we have not stretched specific sections with different values. The correlations were calculated using the standard method and so the number of degrees of freedom is n-2. All alpha values are 0.05 and we have therefore removed them from the text. Instead we indicate the degrees of freedom (n-2) for all correlations in this section.

Obs. 4:

The authors write: "The latter indication is well supported by the high accumulation rate in the region that does not allow a prolonged exposition of the freshly fallen snow to the atmosphere. Furthermore, the absence of significant infiltration and percolation associated with melting and refreezing events and the lack of a relationship between ice layers and seasons as well as with the stable water isotope record implies that the isotopic composition is not altered by surface melt infiltration and percolation". The authors should show the melt percentage per depth, ice layer distribution and thickness in a plot. If they have the data, I do not see the problem on doing it. Including these data in the manuscript will improve and give support to this part of the discussion. As it is, I am still not convinced by the authors' claims, basically because they do not show the data. If the melt layers are "few" why not to simply indicate how many per mwe the cores have? And then calculate melt percentage. In the previous revision of this manuscript, I've asked: "how the authors could explain the melt layers then if there is no signal of infiltration or connection with summer melt? Could the authors include the percentage of melt per m w.e.?" The authors response was: ANS. 12-20. In this line we expressed our self not right. We actually don´t mean to state that a proper ice layer could form purely from wind in a high accumulation region like the AP. We refer here to actual glazed (ice) "crust", only a few mm wide as shown by the stratigraphy of the firn cores. This wind crust could form a thin glazed surface due to sublimation and snow drift abrasion, and in some opportunities by solidification of super-cooled droplets flowing against ground surface irregularities (sastrugi-like). During our field work, we witness these processes during different years. However, in the authors response + corrections uploaded on 2017-09-11, I still see the phrase: "Thus, this reassures that post–depositional processes in the LCL region are negligible in the time period analyzed and that ice layers likely developed by wind ablation on wind–scouring processes at the plateau." Therefore, the authors did not include the clarification in the paper.

Response:

In this reviewed version we include percentage melt, as we agree with the reviewer that this is necessary information to show that melting is not an important with relation to the high accumulation of this region. Nonetheless, we think a new figure is not absolutely necessary, since the melt events are very restricted and not regularly distributed (i.e.: Seasonal distribution). This manuscript has already several figures and the authors consider that, this figure in particular doesn´t contribute vital information to the discussion. Melt percentage were calculated taking in account only, regular and thicker ice layer. Thinner (<1 mm to 1 cm) and irregular glazed crusts are not taken in account in this calculation, as they don´t represent melt, but wind-scouring and droplets solidification.

We will add our previous explanation to the processed, as we recognized that we failed to make it clear as the reviewer correctly points that out. Explanation and correction where added to section 4.2.1 (p. 10, l. 296-304) and section 5.1 (p. 14, l. 439-444)

Obs. 5:

(In 10. 31.) Please define what are "elevated values". A value higher than the mean could be simply a number 1*10^-8 above the mean, but that would not make sense to interpret as a result of a geophysical process, at least not in the manuscript context. Please define higher (or lower) values in terms of how many standard deviations the value is above or below the mean. Please revise the discussion from section 4.2.2 on, considering the above.

Response:

To make this section of the discussion clearer, we remove the term “elevated values” and have modified this phrase to read: “This pattern is characterized by positive monthly mean δ18O standardized anomaly values (z = observation - mean * Std. dev.-1) between May and November in the years 2008 (z = 0.6), 2010, 2012 and 2014 (z > 1). Additionally they exhibit a negative correlation to temperatures at BE (z = -0.7 for 2010, and < -1 for 2008, 2012 and 2014). Between June and July in the following years 2009, 2011 and 2013, δ18O values (z < -1) are lower than the mean and exhibit a positive correlation to temperature at BE (z < -1) (Fig. 9)”. This enables improved understanding of the periodical pattern identified, and a better introduction to Figure 9. The discussion in section 4.2.2 is still consistent with the previous statement.

Minor comments

6. 30-34. Please indicate in the text how you have assessed that there is a significant difference in the Sdev of the cores.

Response:

This is now included: “there was a significant difference in the standard deviation (Sdev > 1.0) of high resolution (5 cm) oxygen isotopes values ”.

7.20-23. Please re-write this sentence: “By studying the progression of these variations, the frequency of the second mode showed the highest frequency in the second interval, where the Sdev reaches an equilibrium. Thus, the final signal is only defined by a set of low frequencies.”, e.g. By studying the progression of these variations, the frequency of the second mode showed the highest value in the second interval, where the Sdev stabilizes?. Thus, the final signal is only defined by a set of low frequencies.
In table 2 please write the mean, max and min values according to the sdev significant digits. Please revise this along the text and tables.

Response:

The first paragraph and the whole section have been revised. Significant digits of values within all tables and within the text have been corrected.

8. 11. The discarding of outliers should be described here, not in the following section (4.1.2.)

Response:

In the revised version, this section was moved from Section 4.1.2. to Section 4.1.1.

8. 24. Please indicate the standard error in the slope of the linear regression when using the MAM and SON datasets.

Response:

A new table (Table 3) including information of the linear regression was now included.

9. 8. "and show variability". This sound ambiguous, please elaborate on this.

Response:

The whole paragraph has been now rewritten and this phrase has been removed.

10. 26-29. If the authors have the number and thickness of ice layers, and layer densities, please include the percentage of melt per m w.e. Without this calculation, this paragraph does not support itself. This was asked in the previous revision and the authors response was that they will include this discussion, however they didn't calculate melt percentage, nor justified why they didn´t do it. In the previous revision, I asked the authors: "how the authors could explain the melt layers then if there is no signal of infiltration or connection with summer melt?" this has not been answered yet. Consequently, the phrase "(10. 26-27) The melt layers do not show evidence of infiltration" remains obscure. This must be clarified.

Response:

This information has been included in Sections 4.1.2 and 5.1. Our observations are based on visual inspection and density profiles of the cores. We defined two different types of high density layers (ice layers and crusts), which were defined based on morphology, and continuous, regular layers thicker than 1 cm are associated to melt events. The thickest layer identified is approximately 5cm, and has defined borders. This implies that these events were not extended in time. Other high density structures which are relatively thin (less than 1 cm) and irregular were associated to other phenomena such as wind-scour ablation and super-cooled droplet solidification. These observations are now stated in the text.

12. 29. Please indicate if the trend is significant and at what confidence level.

Response:

The information is now included in this section and stated as: "A marked decrease was observed in the accumulation during JJA and SON between 2008 and 2015, which could be in part responsible for the overall decreasing rates. However, this trend was found to be statically non–significant (p>0.1)"

13. 10. "During MAM a clear decrease of δ18O with height (-2.4‰ km-1 from sea level at OH up to LCL) is found, whereas during JJA no decreasing δ18O trend is obtained from sea level to 1130 m a.s.l. (Fig. 13b).". Please define the significance of the trend, otherwise, the sentence is ambiguous.

Response:

This was now included as: "Between OH (0 m a.s.l.) and LCL (1130 m a.s.l.) during MAM, a clear decrease of δ18O with height is observed (-2.4‰ km-1 with R=0.97 at p level<0.05), whereas during JJA no significant decreasing δ18O trend is observed (Fig. 14b)"

14. 14. Here I am confused because the editor had already asked to correct the terms “inverse and direct relationships”, however, I still find them in the text, despite the fact the authors claim, in the response to the editor, to have revised them.

Response:

We regret this oversight in the previous version of the text. We have reviewed the text carefully, and made the respective modifications.

2. 3. Warming of

Response:

Corrected as suggested

2. 12. At an estimated rate of

Response:

Corrected as suggested

2.13. Please indicate the rate of positive mass balance in East Antarctica

Response:

Information from Harig and Simmons (2015) has been included, and the section now reads: The glaciers of the AP have lost ice mass at a rate of approximately 27 (±2) Gt y-1 between 2002 and 2014. This mass loss combined with the mass loss over the West Antarctic ice sheet (121(±8) Gt y-1), surpassed the mean positive mass balance of +62 (±4) Gt y-1 observed in East Antarctica, of which most of the positive balance relates to the Dronning Maud Laud region whereas the mass balance of the rest of the EAIS is at equilibrium (Harig and Simons, 2015).

4.6-7. Please cite the ice-core studies that are available.

Response:

The following references are now included: Aristarain et al, 2004; Simoes et al, 2014; Goodwin et al, 2015; Fernandoy et al, 2010, Dalla Rosa, 2013

4.16. Eastern side

Response:

Corrected as suggested

4.30. The authors mention “improper storing” without describing what is proper storing. See also the general comments.

Response:

Additional information is now included: “The overwintering crew at O’Higgins Station collected daily precipitation samples from pluviometers installed at the meteorological observation site. Each daily sample comprised of a filling a narrow neck HDPE type bottle with a 30 ml composite sample of the precipitation (both liquid and solid) that fell in the previous 24 hours. The bottles were tightly closed and stored frozen year–long to ensure correct storage and to facilitate the subsequent transport to the laboratory at the end of each year. From these samples, approximately 6% (13 samples) were discarded from the analysis due to improper storage causing leakage from the bottles. Improper storage was assessed using a statistical outlier test (modified Thompson tau technique) which indicated unusual values of stable water isotope analyses.”

5.4. Please indicate the temperature at which the cores were kept in the commercial freezer.

Response:

The information was now included: “and later transported and stored at -20°C in a commercial cold store in Viña del Mar, Chile.”

In Fig. 2, please indicate the resolution of the meteorological data.

Response:

The information is now included; all data sets correspond to monthly means from the meteorological observatory at Bellingshausen Station.

8. 6. In the last - in the previous

Response:

This was rephrased to read: “across the Bellingshausen Sea during the 24 hours before the air parcels reach the AP (Fig. 5).”

8. 10. Was constructed - was obtained

Response:

Corrected as suggested

10. 17. “an even higher” - a higher

Response:

Corrected as suggested

10. 20. “more fresh and less compacted”. This is ambiguous. If the authors have layer density, please indicate it, e.g. consist of snow layers with density between xx and xx, and firn with densities between xx and xx.

Response:

This information is now included and the section reads: For the overlapping time interval in OH-9 and OH-10 (February 2012 to January 2014), we only considered data from OH-9, as these samples consist of fresher snow layers with density between 350 and approximately 410 kg m-3 (at core depth between 0 and 1 m), and firn with densities between approximately 410 and 530 kg m-3 (at core depth between 1 and 7 m) than the corresponding interval in OH-10.

Observations by Reviewer 2

I thank the authors for addressing many of my concerns in their updated manuscript. It is much improved from the previous version.

Obs. 1:

One main concern I still have is dating the core by peak matching dexcess_core with dexcess_meteo. The authors describe this on page 10 of the revised manuscript around line 10 as “peak-valley fitting”. My understanding is that the authors then present the correlation between the peak-matched datasets as a validation of the dating method. My original point is that this seems circular – we should expect the dexcess in the core and the observations to match since they’ve been aligned. I also agree with the Editor’s comment about artificially increased correlations due to smoothing of the time series. There’s a need to account for reduced degrees of freedom in testing the significance. While the authors now present t-statistics in their revised manuscript, it’s not clear that these were calculated using reduced degrees of freedom (not just n-2) as the editor suggests doing. Perhaps the method presented by Bretherton et al 1999 (J. Climate) would be appropriate here, where an effective sample size (n*) is calculated by accounting for lag-1 serial correlation in time series, and from which to effective degrees of freedom, and then t and p values are calculated.

Response:

As exposed to the observation to the Editor and Reviewer 1 comments, in this version, we improved the description of statistical treatment, that we clearly didn´t correctly expressed in the previous version of this manuscript. We regret, that we didn´t achieved that before and probably caused some confusion to the reviewer. We apologize for this in advance.
As expressed to the Editor in his first observation:
Sections 3 and 4 were rewritten and reformulated accordingly and the focus of the analysis was modified. With these changes we aim to emphasize that the analysis using FFT aimed to extract low frequency oscillations from a noisy signal obtained from the isotope record. The filtered signal was then compared with meteorological data retrieved from re-analysis data using a linear regression analysis. The linear regression model was fitted to the whole data set and in this way

the signal was transformed from the space domain (depth) to the time domain (age). Thereafter temperature, accumulation rate and environmental conditions trends were reconstructed.
Moreover, in response to the Editor´s observations to sections 3 and 4:
This section has been rewritten to make it clear that the stretching value we found via the comparison with the modeled d-excess has been applied to the complete dataset, we have not stretched specific sections with different values. The correlations can therefore be calculated using the standard method and the number of degrees of freedom is n-2. All alpha values are 0.05 and we have therefore removed them from the text. Instead we indicate the degrees of freedom (n-2) for all correlations.

Obs. 2:

The data on figure 4 (the old figure 7) has changed since the last version, substantially in some cases. I am curious why this is. The data now appear to show better correlations.

Response:

The reviewer is right in this point, we unfortunately used an unfiltered data-set to produce the mean monthly values for the first version of the figure. This issue was later corrected, taking out all outlier data points and producing the correct monthly mean values. This didn´t affect any of the statics carried out for this data, since the data-set used for the mathematical treatment was corrected filtered. Therefore, the new version of the figure, offers a better (visual) correlation of the data. The time axis (x-axis) was modified accordingly.

New insights into the use of stable water isotopes at the northern Antarctic Peninsula as a tool for regional climate studies

~~New regional insights into the use of~~Regional ~~stable water isotope~~s ~~signal at the northern Antarctic Peninsula as~~ a ~~tools for regional~~polar ~~climate studies~~

Francisco Fernandoy[1], Dieter Tetzner[2], Hanno Meyer[3], Guisella Gacitúa[4], Kirstin Hoffmann[3], Ulrike Falk[5], Fabrice Lambert[6], Shelley MacDonell[7]

[1]Facultad de Ingenieria, Universidad Andres Bello, Viña del Mar, 2531015, Chile
[2]Center for Climate and Resilience Research, Universidad de Chile, Santiago, 8370361, Chile
[3]Alfred Wegener Institute Helmholtz Centre for Polar and Marine Research, Research Unit Potsdam, Telegrafenberg A43, 14473 Potsdam, Germany.
[4]Programa GAIA-Antártica, Universidad de Magallanes, Punta Arenas, 6210427, Chile
[5]Climate Lab, Geography Department, University Bremen, 28334 Bremen, Germany
[6]~~P~~Department of Physical Geography, Pontificia Universidad Católica de Chile
[7]Centro de Estudios Avanzados en Zonas Áridas (CEAZA), La Serena, Chile~~…~~

Correspondence to: Francisco Fernandoy (francisco.fernandoy@unab.cl)

Abstract. Due to recent atmospheric and oceanic warming, ~~The~~ the Antarctic Peninsula is one of the most challenging regions of Antarctica to understand both local- and regional-scale climate signals~~from a climatological perspective, owing to the recent atmospheric and oceanic warming~~. ~~The s~~Steep topography and a lack of long–term and in situ meteorological observations complicate the extrapolation of existing climate models to the sub-regional scale. Therefore, new techniques must be developed to better understand processes operating in the region. ~~For example, i~~Isotope signals are traditionally related mainly to atmospheric conditions, ~~however,~~but a detailed analysis of individual components can give new insight into oceanic and atmospheric processes. This paper aims to use new isotopic records collected from snow and firn cores in conjunction with existing meteorological and oceanic datasets to determine changes at the climatic scale in the northern extent of the Antarctic Peninsula.

In particular, ~~Here, we present new evidence from the northern Antarctic Peninsula to demonstrate how stable water isotopes of firn cores and recent precipitation samples can reveal climatic processes related to nearby oceanic and atmospheric conditions. A~~a ~~noticeable~~ ~~discernable~~discernible ~~aeffect~~effect of ~~the~~ sea ice cover on local temperatures and the expression of ~~atmospheric~~ climatic modes, ~~in particular~~especially the Southern Annular Mode (SAM), is demonstrated.

In years with a large sea ice extension in winter (negative SAM anomaly), an inversion layer in the lower troposphere develops at the coastal zone. Therefore, an isotope–temperature relationship (δ–T) valid for all ~~seasons~~ periods cannot be ~~concluded~~obtained, and instead,~~.~~ ~~The~~ the δ–T~~. relationship rather~~ depends on the seasonal variability of oceanic conditions. Comparatively, ~~Transitional~~ transitional seasons (autumn and spring) ~~are both stable seasons with an~~have a consistent isotope–temperature gradient of +0.69‰ °C^{-1}. ~~The~~ As shown by firn core analysis, ~~firn stable isotope composition reveals that~~ the near–surface temperature ~~at~~ in the ~~most~~ northern-most portion of the Antarctic Peninsula shows a decreasing trend (-0.33°C y^{-1}) between 2008 and 2014. ~~Moreover~~In addition, the deuterium excess (d_{excess}) ~~has been~~is demonstrated to be a reliable indicator of seasonal oceanic conditions, and therefore suitable to improve a firn age model based on seasonal d_{excess} variability. The annual accumulation rate in this region is highly variable, ranging between 1060 kg m^{-2} y^{-1} and 2470 kg m^{-2} y^{-1} from 2008 to 2014. The combination of isotopic and meteorological data in areas where data exist is ~~a~~ key ~~for~~ to

reconstruct~~ing~~ climatic conditions with a high temporal resolution in ~~polar regions~~Polar Regions where no direct observations exist.

1 Introduction

West Antarctica, ~~and~~ especially the Antarctic Peninsula (AP), has~~ve~~ ~~been in the scope of~~received increasing attention from the scientific community due to the notable effects of ~~the present~~recent warming on the atmosphere, cryosphere, biosphere and ocean. The increase of air temperatures along the West Antarctic Peninsula coast (Carrasco, 2013) displays signs of a shifting climate system since the early 20th century (Thomas et al., 2009). Recently, rapid warming of both atmosphere and ocean ~~is~~ has ~~causing~~ caused ice shelf instability~~ of ice shelves~~ in West Antarctica, especially in some regions of the AP (Pritchard et al., 2012). Instability leading to ~~The collapse of ice shelves triggers~~ice shelf collapse has triggered~~ an accelerated~~ accelerated ice–mass flow and discharge from land-based glaciers into the ocean, as the ice shelves' buttressing function ~~gets~~ is lost. ~~Several grounded tributary glaciers on AP and in West Antarctica recently loose mass to the oceans, and often at a~~Accelerated rates ~~due to this phenomenon~~of ice mass loss (Pritchard and Vaughan, 2007; Rignot et al., 2005; Pritchard et al., 2012), ~~which~~ in combination with increased surface snow melt, has contributed to a negative surface mass balance especially in the northern part of the AP region (Harig and Simons, 2015; Seehaus et al., 2015; Dutrieux et al., 2014; Shepherd et al., 2012).

The glaciers of -the AP have lost ice mass at a~~n estimated~~ rate of approximately~~round~~ 27 (±2) Gt y^{-1} between 2002 and 2014. This mass loss~~, which~~ combined with the mass loss over the West Antarctic ice sheet ~~of (~~(121(±8) Gt y^{-1}~~,~~), surpassed the mean positive mass balance of +62 (±4) Gt y^{-1} observed in East Antarctica, of which most of the positive balance relates to the~~mainly from the~~ Dronning Maud Laud region whereas the mass balance of the rest of the EAIS is at equilibrium (Harig and Simons, 2015). This demonstrates how vulnerable the coastal region of West Antarctica is to increased air and sea surface temperatures (Bromwich et al., 2013; Meredith and King, 2005).

Surface snow and ice melt on the AP represents up to 20% of the total surface melt area (extent) and 66% of the melt volume of whole Antarctica for at least the last three decades (Trusel et al., 2012; Kuipers Munneke et al., 2012). Regional positive temperatures detected by remote–sensing techniques and ice–core data reveal that melt events have been temporally more wide–spread since the mid–20th century (Abram et al., 2013; Trusel et al., 2015), with some severe melt events during the first decade of the 21st century (Trusel et al., 2012). Increased surface melt and glacier calving are likely to have freshened~~may have an impact on the fresh water budget of the~~ upper ocean layers and therefore ~~on~~ impacted~~the~~ biological activity ~~of~~ in the coastal zone (Meredith et al., 2016; Dierssen et al., 2002). The most significant warming trend detected at the coast of the AP ~~occurs~~ occurred during the winter season, especially on the west side of the Peninsula, where a positive trend ~~tendency~~ of >0.5°C decade^{-1} for the period 1960–2000 has been reported at several stations (Turner et al., 2005; Carrasco, 2013). ~~Winter~~ For example, winter warming is especially evident in ~~the~~ daily minimum and monthly mean temperature increases, as described by Falk and Sala (2015) for the meteorological record of the Bellingshausen Station at King George Island (KGI) at the northern AP during the last 40 years. In KGI the daily mean temperature during winter increased at about 0.4°C decade^{-1}, with a marked warming during August (austral winter) at a rate of +1.37(±0.3) °C decade^{-1}. Positive temperatures even in winter are more commonly observed, leading to more frequent and extensive surface melting year–round especially for the northern AP, which is dominated by maritime climate conditions (Falk and Sala, 2015).

The mechanisms ~~behind~~ causing increasing atmosphere and ocean temperatures are still not completely understood but can be ~~confidently~~ linked to perturbations of regular (pre-industrial period) atmospheric circulation patterns (Pritchard et al., 2012; Dutrieux et al., 2014). Most heat advection to the southern ocean and atmosphere has been related to the poleward movement of the Southern Annular Mode (SAM) and to some extent to the El Niño Southern Oscillation (ENSO) (Gille, 2008; Dutrieux et al., 2014; Fyfe et al., 2007). During the last decades, SAM has been shifting into a positive phase, implying lower than normal (atmospheric) pressures at coastal Antarctic regions (latitude 65°S) and higher (atmospheric) pressures over the mid–latitudes (latitude 40°S) (Marshall, 2003). ~~With~~ As a result of lower pressures around Antarctica, the circumpolar westerly winds increase in intensity (Marshall et al., 2006). As a consequence, air masses transported by intensified westerlies overcome the topography of the AP more frequently, especially in summer, bringing warmer air to the east side of the AP (van Lipzig et al., 2008; Orr et al., 2008). The correlation between the SAM and ~~the~~ surface air temperature~~s~~ is generally positive for the AP, explaining a large part (~50%) of near–surface temperature increase for the last half century (Marshall et al., 2006; Marshall, 2007; Carrasco, 2013; Thompson and Solomon, 2002). An enhanced circulation ~~allows~~ enables more humidity to be transported to and trapped at the west coast of the AP due to the orographic barrier of the central mountain chain. ~~Therefore~~This has resulted in the consistent increase of~~, the~~ accumulation ~~has consistently increased~~ across the entire AP~~eninsula~~ during the ~~whole~~ 20th century, thereby doubling the accumulation rate from the 19th century in the southern AP region (Thomas et al., 2008; Goodwin et al., 2015; Dalla Rosa, 2013).

The increase of greenhouse gas concentrations and the stratospheric depletion of the ozone layer, both linked to anthropogenic activity, are thought~~suggested~~ to be the main forcing factors of the climate shift that has ~~affects~~ affected the ocean–atmosphere–cryosphere system for at least the last half century~~-~~ (Fyfe and Saenko, 2005; Sigmond et al., 2011; Fyfe et al., 2007).

The lack of long–term meteorological records ~~hampers~~ limits accurate~~ly~~ ~~determining~~ determination of the onset and regional extent of this climate shift. Therefore, climate models are ~~necessary~~ needed to extend the scarce climate data both spatially and temporally. One major challenge is to correctly integrate the steep and rough topography of the AP into climate models. To facilitate ~~realize~~ this~~ goal~~, ~~direct~~ more detailed information ~~on~~ of surface temperatures, melting events, accumulation rates, humidity sources and transport pathways are urgently needed. As direct measurements of these parameters are often not available, the reconstruction of the environmental variability, basically relies on proxy data such as the stable water isotope composition of precipitation, firn and ice (e.g.:Thomas and Bracegirdle, 2009; Thomas et al., 2009; Abram et al., 2013).

In this ~~investigation~~study, we focus on a stable water isotope–based, high temporal resolution assessment (seasonal resolution between austral autumn 2008 and austral summer 2015) of climate variables including accumulation rates, temperatures and melt events on the AP and their relationship ~~to~~ with atmospheric ~~modes~~ and ~~moisture source~~oceanic conditions i.e. sea surface temperature, humidity and sea ice extent. We investigate the effects of the orographic barrier of the AP on ~~the~~ air mass and moisture transport, with increasing precipitation rates from the coast to the mountain range on the Peninsula divide at ca. 1100 m a.s.l. (Fernandoy et al., 2012), where the ice thickness reaches ca. 350 m at maximum (Cárdenas et al., 2014).

2 Glaciological setting and previous work

Since 2008~~,~~ we have undertaken several field campaigns to the northernmost region of the AP~~,~~ where we have retrieved a number of firn cores of up to 20 m depth. The present investigation is the first of its kind for this sector of the AP. Other studies have been carried out further south at Detroit Plateau (Dalla Rosa, 2013) and Bruce Plateau (Goodwin et al., 2015), at around 100 and 400 km South–West of the northern AP. Nonetheless, not much is known about the glaciological conditions at the northern tip of the AP and very few ice cores have been retrieved from this area despite~~ of~~ the high number of scientific stations in the region (Aristarain et al, 2004; Simoes et al, 2014; Goodwin et al, 2015; Fernandoy et al, 2010, Dalla Rosa, 2013). The AP and Sub-Antarctic islands are principally characterized by mountain glaciers or small ice caps, which flow into the Bellingshausen and Weddell Sea to the West and East, respectively (Turner et al., 2009). Rückamp et al.

(2010), noted that the ice cap covering~~ the~~ King George Island, South Shetlands (62.6°S, 60.9°W) is characterized by polythermal conditions and temperate ice at the surface (>-0.5°C), and is therefore sensitive to small changes in climatic conditions. Further South, Zagorodnov et al. (2012) showed that temperatures from boreholes reach a minimum at 173 m depth (-15.8°C) at Bruce Plateau (66.1°S, 64.1°W, 1975.5 m a.s.l.). Similar glaciological conditions were reported on the east side of the AP at James Ross Island (64.2°S, 57.8°W, 1640 m a.s.l.)~~;~~ (Aristarain et al., 2004). Accumulation rates at the northern AP are directly related to the westerly atmospheric circulation and maritime conditions, with values close to 2000 kg m^{-2} y^{-1} on the west side (Goodwin et al., 2015; Potocki et al., 2016) and lower values (~400 kg m^{-2} y^{-1}) on the E~~e~~astern side (Aristarain et al., 2004); ice thickness from all coring–sites reported is <500 m to the bedrock.

3 Methodology

3.1 Field work and sample processing

During five austral summer campaigns (2008–2010, 2014, 2015), an altitudinal profile was completed from sea level near O´Higgins Station (OH) to 1130 m a.s.l at the Laclavere Plateau (LCL) (Fig. 1). In total, five firn cores ~~were~~ are included in this paper: OH-4, OH-5, OH-6, OH-9, OH-10 (Fig. 1); coordinates and further details of the firn cores are given in Table 1. ~~210~~ Two hundred and ten daily precipitation samples were gathered at the meteorological observation site~~ory~~ of the O´Higgins Station (57.90°W, 63.32°S, 13 m a.s.l.) during 2008–2009 (Fernandoy et al., 2012) and 2014 (Table 2). ~~O~~The overwintering crew at O'Higgins Station ~~gather the~~collected daily precipitation samples from pluviometers installed ~~in a daily base directly from~~at the meteorological observation site~~ory,~~. Each daily sample comprised of a filling a narrow neck HDPE type bottle with a 30 ml composite sample of the precipitation (both liquid and solid) that fell in the previous 24 hours ~~totalizing a daily composite sampling and extracting 30ml sample, that is saved in narrow neck type HDPE bottles~~. The bottles ~~are~~were tightly closed ~~(tighten)~~ and ~~kept~~stored frozen year–long to ensure ~~proper~~correct storage and ~~for~~to facilitate the subsequent~~ later~~ transport~~ed~~ to the laboratory at the end of each year. From these samples, approximately~~round~~ 6% (13 samples) were discarded from the analysis due to improper storage causing leakage from the bottles~~ing, likely due a leak of the bottles~~. Improper storage ~~This~~ was assessed using a statistical outlier test (modified Thompson tau technique) which indicated~~indicated by~~ unusual values of stable water isotope analyses~~, and were discriminated using a statistical outlier test (modified Thompson tau technique)~~.

Cores from the O'Higgins Station site (OH-4, OH-5, OH-6 and OH-9) were retrieved between 2008 and 2010 and analyzed for their stable water isotope composition and physical properties~~ of ice~~ as described ~~in~~by Fernandoy et al. (2012) and Meyer et al. (2000). Additionally, a density profile of OH-9 was obtained ~~by~~ using an X-ray microfocus computer tomograph at the ice–core processing facilities of the Alfred Wegener Institute, Helmholtz Centre for Polar and Marine Research in Bremerhaven, Germany (Linow et al., 2012). ~~The~~ X-ray tomography provides a very high–resolution (1 mm) density profile of the physical properties of the ice. The ~~core~~ OH-10 core was retrieved in 2015 using an electric drilling device with a 5.7 cm inner diameter (Icedrill.ch AG). The retrieved core was first stored under controlled temperature conditions (-20°C) at the Chilean scientific station Prof. Julio Escudero (King George Island) and later transported and stored at -20°C in ~~to~~ a commercial cold stor~~eage~~ in Viña del Mar, Chile. The core sections were measured and weighted for density–profile construction and then sub–sampled to~~with~~ a 5 cm resolution for stable water isotope analysis. A visual log~~ging~~ and description of ~~the~~ each core~~s~~ was~~ere~~ carried out to identify possible melt layers and their thicknesses. Subsequently, the samples were melted overnight at 4°C in a refrigerator at the Stable Isotope Laboratory of the Universidad Nacional Andrés Bello (UNAB), Viña del Mar, Chile. To avoid any evaporation, the 5 cm samples were placed in sealed bags (Whirl-pak) and agitated to~~for~~ ~~homogenization~~ homogenize the samples before isotopic analysis. Firn and~~ recent~~ precipitation samples collected from OH in 2014 (Table 1) were analyzed using~~by~~ a liquid water stable isotope analyzer from Los Gatos Research

(TLWIA 45EP), located at the UNAB facilities. Measurement precision ~~Accuracy of the measurements is~~ was ~~better~~ higher than 0.1 ‰ for oxygen and 0.8 ‰ for hydrogen isotopes for all analyzed samples ~~analyzed~~. All oxygen and hydrogen stable water isotope data ~~of~~ from precipitation and firn core samples are presented in relation to the Vienna Standard Mean Ocean Water Standard (VSMOW) in ‰, as $\delta^{18}O$ and δD for oxygen and hydrogen isotopes, respectively.

3.2 Database and time series analysis

Stable water isotope data were compared to major meteorological parameters from the region (Fig. 2). For this purpose, the following data sets were incorporated into our analysis: daily and monthly ~~Near~~near–surface air temperature (T_{air}), precipitation ~~amount~~ (Pp) and sea–level pressure (SLP)~~,~~ measurements recorded at the ~~Russian Station~~ Bellingshausen Station (BE) (58.96°W, 62.19°S, 15.8 m a.s.l.) and the O´Higgins Station (OH~~,~~). These datasets were downloaded ~~available in daily and monthly resolution~~ from the Global Summary of the Day (GSOD) data sets ~~of~~ from the National Climatic Data Center (NCDC, available at: www.ncdc.noaa.gov) and the SCAR Reference Antarctic Data for Environmental Research (READER, available at: https://legacy.bas.ac.uk/met/READER/) (Turner et al., 2004).

The ~~As~~ temperature ~~data~~ record from OH ~~show~~ contains several large ~~record~~ data gaps, and so the available data from 1968 to 2015 were compared with those measured at BE to evaluate the possibility of lapsing data from BE to the site due to the data continuity available (uninterrupted record since 1968). The BE and OH data are highly correlated ($R=0.97$, $p<0.01$), and so a correction of -1.4ºC was applied to the BE data based on linear regression analysis. ~~we considered the BE temperature corrected by a latitude difference, given by the difference of average air temperature record between OH and BE stations for the common time span from 1968 to 2015 (OH= BE-1.4°C) for all further calculation at OH location, as for the estimation of air temperature on LCL. The BE data was considered for this calculation because of the high correlation with OH (R= 0.97, p<0.01) and long term consistency of the data (uninterrupted record since 1968). The correction is given by the linear regression between OH and BE temperature data.~~ Other nearby stations ~~like~~ such as Esperanza (63.40°S, 57.00°W), were not considered because of a ~~their~~ slightly lower correlation ($R= 0.96$, $p<-0.01$) and ~~likely~~ the possibility of a higher continental influence on the temperature record.

Sea surface temperature (SST) time series were extracted from the Hadley Centre observation datasets (HadSST3, available at: http://www.metoffice.gov.uk/hadobs/hadsst3/). The HadSST3 provides SST monthly means on a global 5° by ~~to~~ 5° grid from 1850 to present (Kennedy et al., 2011a, b). Mean monthly SSTs were extracted from a quadrant limited by 60–65°S and 65–55°W. Missing data or outliers were interpolated from measurements taken in ~~the neighbour~~neighboring quadrants.

Relative humidity (*rh*) time series were extracted from data obtained by the calculation of 3 –day air parcel backward trajectories under isobaric conditions using the freely–accessible Hybrid single-particle Lagrangian integrated trajectory (HYSPLIT) model (http://ready.arl.noaa.gov/HYSPLIT.php). This three–dimensional model was ~~fed with~~run using the global data assimilation system (GDAS) archives from NOAA/NCEP (Kanamitsu, 1989) ~~to~~ at a 1° latitude–longitude spatial ~~coverage~~resolution with a 1 hour temporal resolution and is available from 2006 to present (for more details visit: http://ready.arl.noaa.gov/gdas1.php). For studying the characteristics of air parcels approaching the AP, *rh* time series were obtained ~~considering data~~ from- backward trajectories arriving ~~at~~ under isobaric conditions (850 hPa) at the OH station. SST and *rh* datasets were resampled to a regional scale defined by high–density trajectory paths (Bellingshausen and Weddell Seas). The resampled fields were defined by the spatial coverage of 1 day backward trajectories. The limits of the resulting quadrant extends from 98° W to 34° W longitude and from 47° S to 76° S latitude. The covered area is representative~~ness~~ of the study site~~is area is given~~ because it ~~geographically~~ includes the region affected by westerly winds and sea ice front during winter time, both factors that exert a high influence on ~~the~~ approaching air parcels ~~that approach this region~~. A field horizontal mean of resampled *rh* values between sea level and 150 m a.s.l. was computed ~~in~~ for this area to construct the *rh* time series ~~utilized~~ used throughout this ~~work~~study.

Altitudinal temperature profiles were obtained from radiosonde measurements carried out at BE between 1979 and 1996 (SCAR Reference Antarctic Data for Environmental Research). Lapse rates were calculated from the temperature difference between sea level and the 850 hPa level. SAM index time series were obtained from the British Antarctic Survey (BAS, available at: http://legacy.bas.ac.uk/met/gjma/sam.html) (Marshall, 2003). Mean monthly sea ice extent around the AP (between 1979 and 2014) was obtained from the Sea Ice Index from the National Sea & Ice Data Center (NSIDC, available at http://nsidc.org). The measurements of sea–ice extension incorporated in this study considered as a starting point the coastal location of OH, and the sea–ice front in the direction towards KGI as an end point.

3.3 Stable Isotope time series analysis

Firn and ice cores are often dated by analyzing the seasonality of stable water isotope values. In the firn cores analyzed in this study, ~~T~~there was a significant difference in the ~~S~~standard d~~D~~eviation (Sdev > 1.0) ~~values~~ of high resolution (5 cm) oxygen isotopes values between firn cores from lower altitudes (OH-4, $\delta^{18}O$ Sdev = 1.2) versus cores from higher altitudes (OH-10, $\delta^{18}O$ Sdev = 2.6~~57~~) (Table 1). However, within each individual core, ~~T~~the raw datasets obtained from stable water isotope analysis ~~in firn cores~~ (Section 3.1) produced low oscillation variance in the isotope–depth ~~profiles~~profile. ~~The~~ Whilst the measured isotope signals were ~~considerably~~ noisy, ~~but~~ the values do not fluctuate far from ~~the~~ each core's mean. This low variance, added to the fact that the ~~There was a significant difference in the Standard Deviation (Sdev) values of oxygen isotopes between cores from lower altitudes (OH-4, $\delta^{18}O$ Sdev = 1.2) versus cores from higher altitudes (OH-10, $\delta^{18}O$ Sdev = 2.57) (Table 1). Furthermore, the~~ patterns described in the isotope–depth profiles do not correspond to seasonal cycles, means that dating each core using traditional annual layer counting is complicated~~.~~. ~~Despite several attempts to achieve a chronology by annual layer counting, the noise and the lack of consistent behavior in the isotope signals inhibited this interpretation.~~ Difficulties from using conventional dating methodology for these firn cores led us to search for other ways to define the time scale of our signals.

We first~~ly~~ analysed the d_{excess} data, because d_{excess} is related to seasonal oceanic conditions, and therefore displays an annual signal in this region (Fernandoy et al., 2010). Whilst the stable water isotope results did not display a regular pattern, the d_{excess} is characterized by~~values displayed~~ a noisy, low frequency ~~signal~~oscillation.~~, and so we used a Fast Fourier Transform (FFT) approach to filter the d_{excess} results to extract a seasonal signal. Low frequency data was dated by comparing the filtered, measured dataset with a filtered, theoretical dataset calculated based on atmospheric and oceanic conditions, specifically relative humidity and sea surface temperature, obtained from reanalysis data (GDAS).~~ We use this low-frequency periodic signal to date the core (see below).

We calculated ~~a~~ ~~T~~theoretical d_{excess} values at our site~~was calculated~~ using the relationship between *rh* and SST computed by Uemura et al. (2008): $d_{excess\ meteo}$= -0.42 * *rh* + 0.45 * SST + 37.9. The suitability of using this relationship for the Antarctic Peninsula region was assessed by comparing the d_{excess} measurements of the daily precipitation samples taken at the OH station with the corresponding theoretical values. For each day that a precipitation sample was collected at OH, 3-~~-~~day~~s~~ air parcel backward trajectories were calculated using the HYSPLIT model. We identified ~~F~~frequent air parcel paths ~~were studied~~ and calculated monthly mean values of *rh* and SST from re–analysis data (GDAS) along these paths~~were calculated~~. We found a very good agreement between the measured and our theoretical d_{excess}~~esxess~~ values, with a correlation of R=0.86 (p<0.01)~~XXX~~.

~~Based on the previous significant correlation found between the measured and theoretical d_{excess} values,~~This high correlation allows us to directly compare~~a direct comparison between~~ a synthetic $d_{excess\ meteo}$ time series and the observational d_{excess} record obtained from each firn core~~could be made~~. For the method to be successful, the resultant depth–age model should maximize the common variability between the two time series.

~~Annual chronology was estimated by relating To realize this alternative methodology, the relationship between moisture source conditions and to the isotopic signature of precipitation sampled at the OH station. s was taken into account. Following the previous motivation, f~~~~For each day when that a precipitation sample was collected at OH, a hourly, 3-day air parcel backward trajectoriesy wereas calculated using the HYSPLIT model with hourly resolution. Frequent air parcel paths were studied and monthly mean values of *rh* and SST from re-analysis data (GDAS) along these paths were calculated. Secondly, uUsing the relationship between *rh* and SST calculatedcomputed by Uemura et al. (2008), a theoretical, or synthetic, value of deuterium excess ($d_{excess\ meteo}$) was calculated estimated for the OH station and nearby area (i.e.: northern Antarctic Peninsula) ($d_{excess\ meteo}$= −0.42 * *rh* + 0.45 * SST + 37.9). This allowsenabled a direct comparison between thisa synthetic $d_{excess\ meteo}$ time series and the observational d_{excess} record obtained from the firn cores (d_{excess} = δD − 8 * δ^{18}O). The resultant We look for a depth-age model thatshould maximisesmaximize the common variability between the two .time series.Comparisons were made between the time series model for deuterium excess (d_{excess} = δD − 8 * δ^{18}O), derived from monthly mean values of the OH precipitation isotopic signal, and $d_{excess\ meteo}$, obtained from monthly mean values of *rh* and SST from the southern oceans.~~

~~At the same time, t~~The d_{excess} signal obtained from stable isotope analysis of firn cores ~~was~~is measured ~~represented into a signal~~ with respect to ~~the~~ depth (i.e.: in the space domain). To extract the low frequency seasonal signal we first computed the Fast ~~Fourrier~~Fourier Transform (FFT) of the d_{excess} data, which identifies all the frequencies in the record. The second lowest frequency was the one with~~selected from the FFT process, as it had~~ the highest power~~The second lowest frequency peak was the onethat with the highest power~~. We therefore reconstructed the low~~-~~-frequency d_{excess} signal by calculating the Inverse Fast Fou~~r~~rier Transform (IFFT) from the lowest two identified frequency peaks. ~~The d_{excess} isotope signal, was filtered using the Inverse Fast Fourier Transform (IFFT) in order to transform the space domain (depth) into a frequency representation of the isotope signal. To determine the best frequency of this mode, we analyzed the variation between the original signal and the signal obtained from each step of the Fast Fourier Transform (FFT) decomposition. By studying the progression of these variations, the frequency of the second mode showed the highest frequency, where the Sdev reaches an equilibrium. Thus, the final signal is only defined by a set of low frequencies.~~

~~The theoretical d_{excess} relationship was then used to calculate the behavior of d_{excess} for the length of the reanalysis record (2006 – 2014).~~ We applied the same procedure to the monthly means of the synthetic $d_{excess\ meteo}$ time series, thus obtaining two low-frequency signals that should show the same seasonal variability ~~Thereafter, the same procedure was applied to time series constructed with monthly means of $d_{excess\ meteo}$ described previously. The strong similarities between the two signals,~~ due to their dependency on the same variables (i.e.: environmental condition of the moisture source region). We then chose a linear depth~~-~~-age model that visually matched the variability in the low~~-~~-frequency observational d_{excess} data with the variability in the low-frequency synthetic $d_{excess\ meteo}$ data. ~~In this way , enabled the transformation from the depth domain of the d_{excess} signal (derived from measured stable isotope values) to time. This was made possible by using the common oscillation patterns in both profiles (by their IFFT), as time markers.~~ A single ~~a~~ linear stretching factor was calculated using that relationship and ~~later~~ applied to the ~~whole~~complete firn cores datasets. ~~The results of the dating procedure are shown in Figure 3.~~ We used the same depth~~-~~-age model to put the firn core δ^{18}O records on a time axis for further analysis using monthly means.~~After following this procedure, d_{excess} can be represented by an age model as shown in Fig. 3. Subsequently, monthly means of the firn cores isotope signal were calculated to generate time series for further analysis. Once the d_{excess} signals from firn cores were represented as time series, the same was done for δ^{18}O records, by considering the time–depth constraints defined (Fig. 3).~~

4. Results

4.1 Precipitation samples

Table 2 and Fig. 4 show the stable isotope results, basic statistics and annual distribution of the precipitation samples collected at the OH station~~, respectively~~. Combining δD and $\delta^{18}O$ values from all precipitation samples ~~allows for~~enables the definition of a Local Mean Water Line (LMWL): $\delta D = 7.83 * \delta^{18}O - 0.12$. Backward trajectory analysis of precipitation events reveals high–frequency transport across the Bellingshausen Sea ~~in~~ during the ~~last~~ 24 hours before the air parcels reach the AP (Fig. 5).

4.1.1 Isotope–Temperature relationship

The relationship between the stable water isotope composition of daily precipitation events and daily near-surface temperature (T_{daily}) at OH was assessed using linear regression analysis of a sample set of measurements. The sample population consisted of the months with the largest number of precipitation samples (namely December 2008, March 2008 and 2009, June 2008 and October 2014). Only selected months were analyzed to ensure the most complete set of data within a relatively short timeframe to improve the derivation of the calculated relationship. Outliers, given by anomalous d_{excess} values (see Section 3.1, d_{excess} < -9 ‰), were filtered out in order to avoid disturbances in the model, as the quality of these samples was likely compromised during storage and transport. It should be noted that this relationship will be compared to firn core time series in Section 4.2.2, in order to reconstruct the air surface temperature at Laclavere Plateau.~~With the stable water isotope composition of single precipitation events and daily near–surface temperature (T_{daily}), an isotope–temperature relationship was obtainedconstructed for OH station using linear regression analysis. This relationship will be used later to be compared to firn core time seriess 4.2.2, in order to reconstruct the air surface temperature at Laclavere Plateau. For this purpose, athe sample set for each season was constructedselected from the months with the largest number of samples (i.e. December 2008, March 2008 and 2009, June 2008 and October 2014). The purpose of this selection was to ensure larger datasets within a short period of time, with the aim of showing coherence and relationships between $\delta^{18}O$ and T. The linear regression between $\delta^{18}O$ and T_{daily} based on 208 precipitation events revealed correlation coefficients (R) higher than 0.6 and a statistical significance (p) lower than 0.03 (t-statistic test significant at alpha 0.05). Outliers, given by anomalous Values of d_{excess} (lower than -9 ‰ (see Section 3.1, d_{excess} < -9 ‰), were filtered out in order to avoid disturbances in the model, as the quality of these samples may have been compromised during storage and transport.~~

~~were discarded as explained in section s3.1 and later in 4.1.2. Furthermore~~Additionally, to investigate the ~~same linear regression~~relationship at a monthly scale, a correlation was performed for monthly ~~averages~~ means calculated from daily events (~~$T_{monthly}$;~~ $\delta^{18}O_{monthly}$; ~~)~~$T_{monthly}$) over the 24 month long ~~from the whole~~ precipitation dataset ~~over 24 months~~ (February – 2008 to March – 2009, and April – November, 2014) (~~R= 0.3, p>0.05~~Table3)~~, over 24 months (February – 2008 to March – 2009, and April – November, 2014)~~. Considerable differences were identified between the daily and monthly $\delta^{18}O$–T relationships (Table 3; Fig. 4a), which indicated~~, showing~~ that the isotope–temperature relationship is seasonally–dependent. The seasonality of this ~~trend, can be~~relationship was determined ~~by~~using the linear regression slope (s) of the daily $\delta^{18}O$–T relationship (see Table 3 for statistical details). The seasonal linear regression between $\delta^{18}O$ and T_{daily} based on 208 precipitation events revealed correlation coefficients (R) higher than 0.6 and a statistical significance (p) lower than 0.03. To facilitate the evaluation of seasonal signals, the daily datasets were categorized by season, such that: austral Summer (December-January-February, DJF) was characterized using December 2008 data; austral Autumn (March-April-May, MAM) was characterized using March 2008 and 2009 data; austral Winter (June-July-August, JJA) by June 2008 data; and austral Spring (September-October-November, SON) by October 2014 data. If MAM and SON are combined together, considering they are both shoulder seasons, the ~~of a~~A~~ustral autumn or MAM (March–April–May), considering the March 2008 and 2009 (daily) dataset to be representative of the MAM behavior, has shown to be quite near to *slope* of austral~~

~~spring or SON (September-October-November), considering the October 2014 dataset to be representative of the SON behavior: r= 0.77 (standard error= 2.08, p<0.01) and r= 0.61 (standard error= 2.88, p=0.03), respectively. If only these two datasets (MAM and SON) are taken into account together, a~~ $\delta^{18}O$–T relationship is defined by the ~~new~~ linear regression ~~can be defined as~~: $\delta^{18}O$= 0.79* T_{daily}-7.76 (R= 0.74, p<0.01~~, t-statistic test statistically significant at alpha 0.05~~)~~. Thus, the time series of monthly averages shows a positive correlation between both parameters~~. ~~An inverse behavior of s was identified during July 2008 and June 2014, compared to MAM and SON. Following the same procedure~~For austral Summer, the $\delta^{18}O$–T relationship ~~for, December 2008 austral summer, or DJF (December-January-February), represented by December 2008,~~ can be expressed as: $\delta^{18}O$= 1.17* T_{daeily}-8.19 (R=0.81, p=0.01);~~, was represented by the sample set of December 2008~~ and austral winter ~~or JJA (June-July-August)~~ represented ~~was represented by the sample set of June 2008~~as: ~~, with r values of 1.17 ($\delta^{18}O$= 1.17* T_{daily}-8.19, standard error= 0.62, p=0.01) and 0.35 (~~$\delta^{18}O$= 0.35* T_{daily}-8.66 (R=0.63, p=0.01)~~, standard error= 1.74, p<0.01), respectively~~. ~~Additionally, mean seasonal lapse rates obtained in this region show the highest values during DJF (-5.31 °C km^{-1}), similar values during MAM and SON (4.43°C km^{-1}, and -4.06°C km^{-1} respectively) and the lowest values during JJA (-2.73° km^{-1}) (Fig. 6).~~

4.1.2 Deuterium excess – Temperature relationship

Deuterium excess (dexcess) was calculated for each precipitation sample from stable water isotope data obtained at OH (see Table 2 for descriptive statistics). To evaluate the proximity to the original evaporation source for each precipitation sample, we examined both the isotope-temperature relationship as well as the near surface temperature and d_{excess} relationship using linear regression analysis. ~~Together with isotope–temperature relationship, the relationship of near surface temperature and the secondary parameter d_{excess}, was explored using linear trends to understand the proximity of the evaporation source. From stable water isotope information obtained from precipitation samples gathered at OH, d_{excess} values were calculated for each sample. Table 2 shows d_{excess} basic statistics for the dataset. D~~As for the evaluation of the isotope-temperature relationship (Section 4.1.1), d~~ Values of d_{excess} lower than -9 ‰ (see Section 3.1) were filtered out in order to avoid disturbances in the model, as the quality of these samples may have been compromised during storage and transport. D~~aily d_{excess} values for December 2008, March 2008 and 2009, June 2008 and October 2014~~the same months as specified in section 4.1.1~~ were compared with daily mean temperatures, ~~similar as for $\delta^{18}O$–T. C~~however, correlation coefficients ~~for these comparisons are~~ were not significant (Table 3)~~R>-0.42 and R<0.09, p>0.1, for negative and positive correlation period, respectively) and show variability~~. However, for the 2008-09 datasets ~~Bby~~the d_{excess}–T correlation ~~comparing~~ for monthly ~~temperature~~ averages (calculated from daily events as outlined in Section 4.1.1) ~~to the datasets of 2008–2009 and 2014, the d_{excess}–T correlation~~ was ~~found to be~~ significant (Table 3; Fig. 4b), and the associated ~~defining a~~ linear regression waas calculated to be: ~~coefficient improved (Fig. 4b). For the 2008–2009 dataset, we obtained a correlation coefficient of R= -0.77 (p<0.01; T= -1 *~~ d_{excess} ~~+~~= -0.60 * $T_{monthly}$~~1~~+2.12 (R=-0.77, p<0.01)~~.53; t-statistic test statistically significant at alpha 0.05)~~. For the 2014 dataset the correlation is not significant~~,~~ ~~defining a linear correlation: d_{excess} = 0.65 * $T_{monthly}$+0.94~~ (R=0.33, p>0.05).~~, we obtained an R=0.33 (p>0.05; T=0.17 * d_{excess} – 3.62).~~

4.1.3 Moisture source of precipitation

Three-~~-~~day air parcel backward trajectories from precipitation events exhibit a wide distribution, probably explaining in part the variability of the isotope–temperature relationship presented in Sections 4.1.1 and 4.1.2. Most of the pathways originat~~eing~~ ~~spatially~~ in ~~both~~ the Southern Pacific Ocean and the Amundsen–Bellingshausen Seas. The trajectories are ~~mainly~~ primarily derived from the Bellingshausen Sea, the Bransfield Straight and the Drake Passage, Tierra del Fuego and South America's southern tip. ~~Moreover~~In addition, some trajectories (<15%) originate from AP's eastern side. Precipitation trajectories show a~~nn~~ ~~pattern~~ almost elliptically distributed pattern ~~pattern~~ with a N40°W orientation, ~~where~~ and most follow pathways ~~bounded by the latitudes~~between 60°S and 67°S. The correlation between monthly mean values of

d_{excess} (from precipitation samples) and $d_{excess\ meteo}$ (constructed from the meteorological parameters *rh* and SST of the high density precipitation pathways) had~~, showed~~ a significant correlation coefficient of R= 0.86 (*p*<0.01~~; t-statistic test statistically significant at alpha 0.05~~) (Fig. ~~7~~6), demonstrating that oceanic conditions control most of the precipitation variability~~ as the results of the previous sections pointed out~~.

4.2 Firn core samples from the AP

Table 1 shows the stable isotope results and ~~basic~~ descriptive statistics for firn cores retrieved at the northern AP. The co–isotopic relationship δD–$\delta^{18}O$ ~~of~~ for each single firn core retrieved from LCL is ~~analogous~~ related to the global meteoric water line (GMWL) and the local meteoric water line (LMWL) (Rozanski et al., 1993), with a mean slope of s= 7.91 and an intercept of 3.64 (Fig. 7~~8~~). These values are very close to those of the LMWL, although with a slightly higher intercept.

4.2.1 Age model based on stable water isotopes

Stable water isotope results from each firn core~~s~~ allow ~~to derive~~the derivation of individual depth profiles ~~of~~ of δD, $\delta^{18}O$ and d_{excess} for each firn core. Lowest noise values and the clearest seasonal patterns were found in d_{excess} profiles ($d_{excess\ core}$) (Fig. 3), similar to findings published by Fernandoy et al. (2012). In S~~s~~ection 4.1.3 it was shown ~~how~~that ~~Fernandoy et al. (2012). Due to the, and there was a high correlation between~~ d_{excess} from precipitation samples and $d_{excess\ meteo}$ at sea level~~,~~ are significantly correlated, which~~ and therefore~~ suggest~~ings~~ a nearby moisture source ~~of the moisture~~ precipitating in this area ~~(see section 4.1.3), the correlation between~~ ~~$d_{excess\ meteo}$ and $d_{excess\ core}$ was evaluated~~. The significant correlation ~~points out~~indicates that,~~meant that~~ moisture source ~~the This was done to determine if the~~ conditions of a coastal and oceanic–proximal ~~moisture source~~origin~~, that~~ will be ~~were~~ ~~also~~ represented and preserved in the $d_{excess\ core}$ record~~, and so~~ and could ~~to~~ be used ~~later~~ as a ~~chronology~~ chronological marker. The $d_{excess\ core}$ signals were first filtered for their high frequency oscillation patterns and then the remnant signals were compared with the high frequency filtered $d_{excess\ meteo}$ monthly means (See S~~s~~ection 3.3). The ~~inter~~comparison between $d_{excess\ meteo}$ and $d_{excess\ core}$ ~~illustrates~~ resulted in a close similarity between them. Main peak–valley fitting between both signals le~~a~~d~~s~~ to a monthly mean $d_{excess\ core}$ signal represented on a defined depth~~–~~–time scale (Fig. 8). The comparison between time series of monthly mean $d_{excess\ core}$ and $d_{excess\ meteo}$ data reveals correlation coefficients of R≥0.67 (*p*<0.01;~~–~~ degree of freedom (df) > 21 for all single cores, see table 4) ~~t-statistic test statistically significant at alpha 0.05)~~ for all firn cores analyzed and obtained from 2006 to 2015. Table ~~3~~4 summarizes correlation coefficients, statistical significances and time intervals for each firn core. From the firn cores retrieved from LCL, a single time series was constructed ~~-~~and then compared to the $d_{excess\ meteo}$ time series in order to analyze the isotopic signal for the whole time interval. A ~~n even~~ higher correlation coefficient of R= 0.75 (*p*<0.01; df= 81~~t-statistics test statistically significant at alpha 0.05~~) was obtained between the two signals ($d_{excess\ meteo}$ and $d_{excess\ core}$). For the overlapping time interval in OH-9 and OH-10 (February 2012 to January 2014), we only considered data from OH-9, as these samples consist of ~~more recent~~~~fresh~~fresher snow layers with density between 350 and ~~around~~approximately 410 kg m^{-3} (at core depth between 0 and 1 m), and firn with densities between ~~around~~approximately 410 and 530 kg m^{-3} (at core depth between 1 and 7 m) ~~and less compacted firn~~ than the corresponding interval in OH-10. This in turn helps to avoid attenuation of the isotopic signal. Although we only considered OH-9 data for the overlapping time interval, we studied the changes in the standard deviation of the isotopic signal ($\delta^{18}O$ and δD) from both firn cores in the common time span. The standard deviation shows a decrease of 16% after one year of deposition in core OH-10 with respect to the same time interval in OH-9; and for 2 to 3 years after~~ the~~ deposition, the standard deviation of the signal decreases by 18%.

During visual firn core logging and density ~~determination~~measurement, thin and scarce elevated density ~~melt l~~layers were identified. Melt layers were characterized by regular lateral extension and thickness 10 mm or higher. A 50 mm thick layer ~~of around 50 mm of thickness~~ was observed in the core OH-10 at depth 8.5m, ~~showing~~which was the maximum observed thickness~~ observed~~. Melt ~~add up~~represented a total of 5% of the accumulated water equivalent column of the cores OH-6, OH-9 and OH-10. The melt layers do not show clear evidence of infiltration nor have a clear pattern of distribution with depth (i.e. an association with summer layers, as there are more or less homogenously distributed along the cores). Other firn high density structures, such as~~,~~ thinner crust like layers (<10 mm), do not correspond to melt events and are mostly related to wind scour processes and liquid precipitation~~ of liquid droplets (mean width of ~1 cm)~~. ~~The melt layers do not show evidence of infiltration nor have a clear pattern of distribution with depth (i.e. the~~ an ~~association with summer layers).~~ Melt and crust layers do not show a clear seasonal pattern with relation to ~~While analyzing the melt layers in relation to~~ their time equivalent with depth~~, no clear pattern associated with a season was noted~~. Around 70% of melt layers counted have a width <10 mm.

4.2.2 Seasonal temperature reconstruction from stable water isotopes

The age model developed using the $d_{excess\ core}$ oscillation was later applied to construct a $\delta^{18}O$ time series (Fig. 3). From this time series a periodical two~~2-~~year pattern was identified. This pattern is characterized by ~~elevated values,~~a positive monthly mean $\delta^{18}O$ standardized anomaly~~ higher than the $\delta^{18}O$~~ values (z = observation - mean * Std. dev.$^{-1}$) ~~monthly mean values~~ between May and November in the years 2008 (z = 0.6), 2010, 2012 and 2014 (z > 1~~),~~). Additionally, they~~which~~ exhibit a~~n~~ ~~inverse relationship~~negative correlation to temperatures at BE (z = -0.7 for 2010, and < -1 for 2008, 2012 and 2014). Between June and July in the ~~following~~ years 2009, 2011 and 2013, $\delta^{18}O$ values (z < -1) are lower than the mean and exhibit a ~~direct relationship~~positive correlation to temperature at BE (z < -1) (Fig. 9~~9~~). Therefore, the two~~-2~~ year periodical pattern mentioned above is represented by even numbered years with austral W~~w~~inter $\delta^{18}O$ values higher than the mean, followed by odd numbered years with austral winter $\delta^{18}O$ values lower than the mean. Monthly mean $\delta^{18}O$ values were transformed to their temperature equivalent using the $\delta^{18}O$–T relationship obtained in S~~s~~ection 4.1.1 from precipitation samples (Fig. 10~~10~~)~~, in order~~ to investigate their seasonal behavior.

Calendar seasons in these latitudes do~~es~~ not follow regular patterns (i.e. DJF, MAM, JJA, SON), as seasonality largely depends on the sea ice cover during winter, often extending beyond ~~their~~ calendar limits. Large sea ice extent (SIE) leads to a delayed on–set of spring conditions. In this case winter–like conditions will be extended beyond August. Restricted sea ice extent on the contrary will lead to earlier S~~s~~pring–like conditions (before August). Depending on ~~this~~ such conditions, we defined three seasons with their corresponding $\delta^{18}O$–T relationship. These seasons are: (1) an austral transitional season which considers the months from March to May and October–November (MAM-ON) (using precipitation datasets from Table 3, March 2008–2009 and October 2014 for the $\delta^{18}O$–T relationship~~ during that season, s=0.69~~), (2) an austral W~~w~~inter season which considers the months from June to September (JJAS) (using precipitation datasets from June 2008 for the $\delta^{18}O$–T relationship, Table 3~~ during that season, s=0.35~~), and (3) an austral S~~s~~ummer season which considers months from December to February (DJF) (considers precipitation datasets from December 2008 for the $\delta^{18}O$–T relationship~~ during that season, s=1.17~~). All ~~(compare of this section refers to the $\delta^{18}O$–T relationship functions in section 4.1.1). Despite t~~This ~~main~~ basic ~~seasonal~~ classification of the seasons to~~for the use of~~ describe the $\delta^{18}O$–T relationship does not explain all of the variability observed in the data, some particular seasons showed variable behavior when compared to the mean seasonal behavior in the time span covered in this study. In those cases, the seasonal behavior was extended or contracted beyond the boundaries of the main season classification depending on the SIE.

4.2.3 Air temperature trends at Laclavere Plateau

In the AP region, lapse rates change seasonally primarily due to variations in the presence and extent of sea ice cover which impacts thermal stability on the lower atmosphere. M~~To reconstruct the near surface temperature from isotope data retrieved from firn cores and meteorological data from near stations, conditions of thermal stability of the lower atmosphere was~~

~~explored throughout different seasons. In the same way as for seasonality of the isotope–temperature relationship, mean~~ seasonal lapse rates obtained in this region show a clear seasonal dependency, with the highest rates during DJF (-5.31 °C km^{-1}), ~~alike~~similar values during MAM and SON (-4.43°C km^{-1}, and -4.06°C km^{-1} respectively) and the lowest rates during JJA (-2.73° km^{-1}) (Fig. 11).

Monthly near surface temperatures at LCL were estimated using ~~Therefore,~~ ~~U~~ua linear regression analysis based on ~~sing the linear correlation between meteorological data:~~ monthly lapse rates in BE, winter SAM index and SIE from OH (Fig. 1~~1~~2~~),~~). The resultant equation is:~~a monthly temperature mean estimate that can be expressed by the equation~~ T_{LCL}= (T_{BE} -1.4)+1.13 (M_{month}*SIE_{OH}+N_{month}), during the months when sea ice is developed (from May to September) and where M_{month} and N_{Month} represent the slope and intercept of the monthly lapse rate–SIE relationship, respectively. During the months when there is no sea ice (from October to April) the monthly temperature ~~can be expressed by the equation~~is calculated from T_{LCL}= (T_{BE} -1.4)+1.13 * H(t), where H(t) is the monthly mean lapse rate value of the month t measured in BE between 1978-1996. Considering th~~ei~~se variables, a mean annual air temperature of -7.5°C with a trend of -0.18°C $year^{-1}$ (statistically not significant at p=0.05) was estimated ~~on~~ for LCL for ~~the time period~~ 2009-2014. ~~On the other hand,~~Comparatively, ~~considering~~ if only the $\delta^{18}O$ time series data and the isotope–T relationship are considered, a mean annual air temperature of -6.5°C with a trend of -0.33°C $year^{-1}$ (statistically not significant at p=0.05) ~~was~~ is estimated ~~on~~ for LCL for the ~~years 2009-2014~~same period. The ~~comparison~~ correlation between monthly mean temperature ~~on~~ at LCL, estimated using the $\delta^{18}O$ signal from firn cores and T_{LCL} estimated using the coupled effect of the latitude–corrected temperature record from BE, SIE_{OH} and lapse rates from BE, ~~reveals~~ have a correlation coefficient of R= 0.70 (p<0.01~~; t-statistics test statistically significant at alpha 0.05~~). Both signals show a synchronous behavior, also with respect to the air temperature recorded at OH station. No statistically significant ~~direct~~ correlation was observed between coastal stations (OH and BE) temperature records and the stable water isotope composition of firn cores.

4.2.4 Accumulation rates

Density measurements from firn cores were used to construct density–depth profiles. Along these profiles a significant increase of density with depth was obtained. Linear regressions across different sections represent a normal firn compaction process reaching the snow–firn–density boundary (550 kg m^{-3}) at the 15.2 m depth. Using these linear regressions and considering the depth intervals delimited in S~~s~~ection 4.2.1 as monthly values, we were able to estimate accumulation rates for different years. ~~By using this procedure, we have estimated a~~A mean accumulation rate of 1770 kg m^{-2} y^{-1} was estimated at LCL ~~between~~ for 2008 ~~and~~ to 2015. The highest accumulation total was found in 2008 (>2470 kg m^{-2}), ~~then~~ and the ~~rate~~ amount noticeably ~~decreased until~~reduced until 2015 (1600 kg m^{-2}) with ~~its~~ an absolute minimum recorded in 2010 (1060 kg m^{-2}) (Fig. 1~~2~~3a). ~~The~~A ~~stronger~~marked decrease ~~A seasonal trend~~ was observed~~,~~ ~~reflecting a decrease~~ in ~~the~~ accumulation ~~rates~~ during JJA and SON between 2008 and 2015, which could be in part responsible for the overall decreasing rates. However, this trend was found to be statically non–significant (p>0.1)~~, which is responsible for the overall decreasing rates~~. ~~On the other hand, t~~The highest accumulation occurs during the MAM and SON seasons (Table 4~~5~~). Accumulation rate estimations derived from the ~~cores~~ OH-9 and OH-10 cores for the common period ~~in~~ 2012 – 2013 only differ ~~only~~ by ~~about~~ approximately 3%. Other cores from the western flank of the Peninsula (OH-4, OH-5 and OH-6) show that the accumulation in 2008 (common period) depends on ~~the~~ altitude, with increasing values from the lower region to the highest point on the LCL (Fig. 1~~3~~2b). The ~~increase~~ rate of increase was ~~about~~ aproximately 1500 kg m^{-2} km^{-1} y^{-1} from 350 m a.s.l. to 1130 m a.s.l. in 2008.

5 Discussion

5.1 Stable water isotope fractionation and post–depositional processes ~~processes and the local temperature relationship~~

The stable water isotope composition of precipitation samples from the 2008 and 2014 datasets ~~show a high interannual~~ are very similar~~ity~~ to each other, ~~as well as~~and to firn cores from the western flank and from LCL Plateau ~~at AP~~ (OH-4 to OH-10). Comparing the $\delta^{18}O$ signal from OH-6 with data from precipitation samples at OH and with two other cores from the western side of the AP (OH-4 and OH-5) during a common period (March 2008 – August 2008), a $\delta^{18}O$ decrease of -0.085‰ km^{-1} was found with increasing distance from the coast (Fig. 14~~3~~a). The same data set was used to study the $\delta^{18}O$–altitude relationship. The $\delta^{18}O$ seasonal means show an altitude dependency that yields seasonal $\delta^{18}O$–altitude patterns. Between OH (0 m a.s.l.) and LCL (1130 m a.s.l.) ~~During~~ during MAM, ~~-~~a clear decrease ~~from sea level at OH up to LCL~~ of $\delta^{18}O$ with height is observed (-2.4‰ km^{-1} with R=0.97 at p level<0.05~~from sea level at OH up to LCL~~) ~~is found~~, whereas during JJA no significant decreasing $\delta^{18}O$ trend ~~(statistically not significant)~~ is observed~~tained~~ ~~from sea level to 1130 m a.s.l.~~ (Fig. 1~~3~~4b).

~~Moreover, further agreement can be found to several meteorological and climatic parameters as well as to reanalysis data.~~ Backward trajectory analysis revealed that the most frequent pathways for air parcels that reach the northern part of AP derive from the Bellingshausen Sea, between 55°S and 60°S ~~(Fig. 5)~~ throughout the year (Fig. 5). In contrast, localities further south on the AP and in West Antarctica, Ellsworth Land and coastal Ross Sea, respectively, exhibit a stronger continental influence on the precipitation source, depending on seasonal and synoptic scale conditions (Thomas and Bracegirdle, 2015; Sinclair et al., 2012). The LMWL obtained from precipitation samples at OH (m= 7.83) is similar to the Antarctic meteoric water line obtained by Masson-Delmotte et al. (2008) (m= 7.75), and to the GMWL as presented by Rozanski et al. (1993) (m= 8.13). The similarity between the slope of LMWL and GMWL indicates that the fractionation processes during condensation mostly take place under thermodynamic equilibrium (Moser and Stichler, 1980). These results are consistent with those obtained by other authors for King George Island (Simões et al., 2004; Jiahong et al., 1998). Combining the stable water isotope signature of OH precipitation with time series of meteorological data representative for the conditions prevailing on the ocean near the OH station, a strong relationship with *rh* and SST at the moisture source can be derived. This relationship has been well established, especially for the coastal Antarctic region where moisture transport from the source is generally of short–range~~ing~~ (Jouzel et al., 2013). The correlation between the d_{excess} of precipitation and a theoretical $d_{excess\ meteo}$ derived from time series of meteorological data from the surrounding region has shown that both datasets are highly correlated (R= 0.86). Based on this evidence, we ~~suggest~~ propose that the Bellingshausen Sea constitutes the most important source of water vapor for precipitation for the study region at the northern AP. A similar conclusion was drawn for regions further south at the Peninsula (Thomas and Bracegirdle, 2015), however, with an increase of contributions from other local sources (e.g.: Amundsen Sea and continental conditions) to the local precipitation. This has also been observed at the northern AP, where some precipitation events that exhibited a stable water isotope composition beyond the normal range for the region (e.g. 20 August 2009, $\delta^{18}O$ = -19.4‰), were associated with uncommon sources of humidity as ~~also recognized~~shown by the backward trajectory analysis.

In firn cores obtained from the AP, average values from both $\delta^{18}O$ and δD decrease as elevation increases to LCL (1130 m a.s.l.), which supports the altitudinal isotope effect identified by Fernandoy et al. (2012) for the region. In addition, standard deviations of seasonal (monthly mean) δD and $\delta^{18}O$ values of firn cores from LCL are low and similar to those of firn cores from lower altitudes. Despite the variations in isotopic composition with height, in all firn cores the δD–$\delta^{18}O$ co–isotopic correlation is very similar to the LMWL obtained from precipitation samples at OH. This provides evidence of the uniformity of the fractionation conditions during the condensation process. Although a slight isotopic smoothing effect was distinguished between the cores (16% after one year of deposition), the distortions caused by post–depositional effects that may alter or homogenize the isotopic signal at this site, such as diffusion, can be considered as limited. The latter indication is well supported by the high accumulation rate in the region that does not allow a prolonged exposition of the freshly fallen snow to the atmosphere. Furthermore, the absence of significant infiltration and percolation associated with melting and refreezing events and the lack of a relationship between ice layers and seasons as well as with the stable water isotope record implies that the isotopic composition is not altered by surface melt infiltration and percolation Thus, this reassures that post–depositional processes in the LCL region are negligible in the time period analyzed. High firn density peaks, mostly thinner than 10 mm, are represented by discontinuous or non–regular layers and counts for 25% of the total layers. These layers developed by wind ablation on wind–scouring processes, when the air and drifted snow flows against surface irregularities (like Sastrugies); and also by solidification of super–cooled droplets. In both cases, a thin ice crust was formed, as observed during the field seasons and in the core stratigraphy. Melt events, recognized by more regular and thicker firn and ice layers (>10 mm), represent approximately 75% of total high density layers (See Section 4.2.1). Even though these observations are in agreement with the results obtained in this region by Fernandoy et al. (2012) and Aristarain et al. (1990), several studies (Fernandoy et al., 2012; Simões et al., 2004; Travassos and Simoes, 2004; Jiahong et al., 1998) have identified a significant melt layers in firn cores, mainly from KGI and from the western side of the AP at altitudes below 700 m a.s.l. The limited effect of post–depositional processes due to the high accumulation rates and to the ice layers reducing diffusion (Stichler et al., 2001), along with the high correlation between $d_{excess\ meteo}$ and d_{excess_cores}, confirm that the isotopic variations observed in firn core isotope records are mostly related to isotopic fractionation occurring during condensation and to *rh* and SST conditions in the vapor source regions.

5.2 Stable water isotope and the local temperature relationship

The changing seasonal $\delta^{18}O$–T relationship obtained from precipitation samples shows that the relationship between air temperature and condensation temperature varies throughout the year. The strong similarity in the $\delta^{18}O$–T relationship during MAM and SON contrasts with the pronounced difference of this relationship between DJF and JJA. This highlights the variability of the $\delta^{18}O$–T relationship along the whole year at the northern AP. ~~Although~~ However, the $\delta^{18}O$–T correlations~~,~~ presented in this study~~,~~ were calculated from precipitation samples of particular months and years, which can ~~certainly~~ induce ~~some~~ bias. However, it can be assumed that~~considering~~ these datasets give an~~ rough~~ idea of the variations that can be seen in between seasons in this region. Furthermore, the $\delta^{18}O$–T correlations obtained for MAM and SON (0.77‰ °C^{-1}and 0.61‰ °C^{-1}, respectively) are similar to the values obtained by other authors for the AP (Aristarain et al., 1986; Peel et al., 1988). Even though the ~~considered~~ dataset is capable of representing variations within the time span covered by this study, it is too short to build a consistent baseline for the region. Despite the reduction of the seasonal temperature difference ~~is reduced~~ in coastal sites, the difference in the seasonal $\delta^{18}O$–T relationship suggests the existence of processes that disrupt the direct linkage between condensation temperature and surface air temperature. The ~~inverse relationship~~negative correlation between the $\delta^{18}O$ signal from LCL ice cores and BE (and OH) monthly mean temperatures (Fig. 9~~9~~ and 10~~10~~), which is noticeable in some years during JJA, contrasts with the commonly accepted seasonal behavior characterized by a ~~direct relationship~~positive correlation between $\delta^{18}O$ and surface air temperatures (Clark and Fritz, 1997). This particular behavior could be related to strong variations in meteorological conditions in the area between BE (OH) and LCL throughout the whole year. Therefore, air temperature on LCL was estimated by two independent methods: lapse rates (vertical temperature gradients) and $\delta^{18}O$–T equivalents. The best correlation between both LCL temperatures estimations was obtained when an extended seasonal behavior was considered (R= 0.70; p<0.01). This result is in agreement with the natural seasonal variability in high latitudes, where the effects of some seasons extend beyond the calendar seasonal temporal limits related to the SIE, as previously explained. Without taking this seasonal variability into account would lead to a misinterpretation of the air temperature reconstruction for LCL, since the $\delta^{18}O$–T correlation would then be rather poor (R= 0.42) and not reflecting the true seasonality in this region. The high similarity in the $\delta^{18}O$–T relationship during MAM and SON can be explained by the seasonal transition between summer and winter, when oceans surrounding the northern AP pass from ice–free to fully ice–covered conditions (or vice versa), respectively. I~~Likely, i~~ce–free ocean conditions are related to seasonal oscillations, which are highly dependent on atmospheric circulation patterns. In this sense, years with a marked negative SAM anomaly are associated with ice–covered sea conditions, whereas positive SAM phases are associated with ice–free sea conditions (Fig. 12~~1~~). Other studies (Turner et al., 2016) point to a similar interaction between surface air temperature and SIE at AP and recognized that the SIE's inter–annual variability is related to atmospheric modes. This supports our own observations ~~in a way~~ that the sea ice is important for regulation of surface air temperatures in the region.

~~In firn cores obtained from the AP, average values from both $\delta^{18}O$ and δD decrease as elevation increases to LCL (1130 m a.s.l.), which supports the altitudinal isotope effect identified by Fernandoy et al. (2012) for the region. In addition, standard deviations of seasonal (monthly mean) δD and $\delta^{18}O$ values of firn cores from LCL are low and similar to those of firn cores from lower altitudes. Despite the variations in isotopic composition with height, in all firn cores the δD–$\delta^{18}O$ co–isotopic correlation is very similar to the LMWL obtained from precipitation samples at OH. This provides evidence of the uniformity of the fractionation conditions during the condensation process. Although a slight isotopic smoothing effect was distinguished between the cores (16% after one year of deposition), the distortions caused by post–depositional effects that may alter or homogenize the isotopic signal at this site, such as diffusion, can be considered as limited. The latter indication is well supported by the high accumulation rate in the region that does not allow a prolonged exposition of the freshly fallen snow to the atmosphere. Furthermore, the absence of significant infiltration and percolation associated with melting and refreezing events and the lack of a relationship between ice layers and seasons as well as with the stable water isotope record implies that the isotopic composition is not altered by surface melt infiltration and percolation Thus, this reassures that post–depositional processes in the LCL region are negligible in the time period analyzed and that ice layers likely developed by wind ablation on wind–scouring processes at the plateaus, aobservLargerpproximatelytotal S. Although Even though these observations are in agreement with the results obtained in this region by $d_{excess\ meteo}$ and $d_{excess-cores}$, confirm that the isotopic variations observed in firn core isotope records are mostly related to isotopic fractionation occurring during condensation and to *rh* and SST conditions in the vapor source regions.~~

5.3~~2~~ Firn age model and accumulation rates

The stable water isotope signal obtained from firn cores shows no regularity in its seasonal behavior and lacks a clear annual oscillation pattern, likely ~~because of~~due to the strong maritime influence (Clark and Fritz, 1997). These two criteria prevent the development of an age model by conventional annual layer counting in the isotope record (Legrand and Mayewski, 1997). In this context, the d_{excess} parameter represents a robust time indicator, as it has shown to be principally dependent on *rh* and SST conditions prevailing in the eastern Bellingshausen Sea where these variables are relatively stable (Jouzel et al., 2013). The high correlation coefficients (and high statistical significance) obtained for the relationship between d_{excess} and $d_{excess\ meteo}$, as shown in ~~section~~ Section 4.2.1, demonstrate that the method used to construct a time series is effective in dating isotope records of firn cores from the northern AP, even at a monthly resolution.

The most frequent d_{excess} values found in the firn cores (3‰ – 6‰) are in agreement with a strong coastal influence scenario as determined by Petit et al. (1991), implying that the d_{excess} relates to *rh* and SST of the humidity source and not to surface air temperature (Jouzel et al., 2013). Saigne and Legrand (1987), postulated that *rh* conditions prevailing at the sea surface have an important effect on the d_{excess} signal of precipitation below 2000 m a.s.l in the study region. The stable water isotope results, in combination with the meteorological datasets ~~records presented in this work~~, show that precipitation on LCL is highly correlated with *rh* and SST conditions in the Bellingshausen Sea near the AP.

The irrelevance of post–depositional effects along with the flat topography on LCL suggests that the estimatio~~n~~e of accumulation rates from firn cores is representative of the amount of snow originally precipitated. Moreover, the slight smoothing of the isotope signal ~~effect~~ after deposition, as well as the small differences in the accumulation rate observed for the common time period of firn cores OH-9 and OH-10, demonstrates that our age model is reliable, as two different data sets yield similar estimations for a common period. The results obtained enable~~allow~~ ~~to classify~~ LCL to be classified as a high annual snow accumulation site (Table ~~4~~5), closely following the estimations of other authors on King George Island dome (Bintanja, 1995; Zamoruyev, 1972; Jiahong et al., 1998) and on the AP further south of LCL (Dalla Rosa, 2013; Goodwin, 2013; van Wessem et al., 2015),~~–~~ of around 2000 – 2500 kg m^{-2} y^{-1}, but differs from the accumulation rate obtained by Simões et al. (2004) and Jiankang et al. (1994) on King George Island dome (600 kg m^{-2} y^{-1}). A seasonal accumulation bias ~~of the accumulation~~ was noted, with more favorable conditions for accumulation (i.e. higher precipitation amount) during autumn resulting from more ~~synoptic scale features~~frontal systems approaching the AP (Table ~~4~~5).

5.4~~3~~ Seasonal variability and disruption of atmospheric conditions

The depletion of $\delta^{18}O$ with increasing height (altitude effect) and the simultaneous increase in accumulation along the western side of AP at the LCL latitude can be explained with the help of an orographic precipitation model as proposed by Martin and Peel (1978). This model states that moist air parcels from the Southern Ocean are forced to ascend and cool down when approaching the AP due to the steep topography forming an orographic barrier to westerly winds. The depletion observed in $\delta^{18}O$ reflects the strength of the fractionation process taking place within a short distance and in a low temperature environment (Fig. 15~~4~~a). Therefore, the isotopic fractionation process occurring at the AP and the direct linear relation between $\delta^{18}O$ and the condensation temperature ~~allow~~ enable us to study ~~the~~ temperature behavior with respect to ~~the~~ altitude increase on the basis of $\delta^{18}O$ variations (Craig, 1961). However, whereas MAM air temperatures show a clear decrease with increasing height (atmospheric instability of the lower troposphere), JJA air temperatures exhibit an increase from sea level to 350 m a.s.l (atmospheric stability). At higher altitudes, a decreasing temperature trend is observed (atmospheric instability). The break at 350 m a.s.l during JJA could indicate the existence of a strong stratification within the lower troposphere on the western side of the AP. In addition, the variations in monthly mean lapse rates measured by radiosondes in BE throughout the year, provide evidence for the existence of a process that modifies the behavior of the lower troposphere, decreasing the lapse rate (between sea level and 850 hPa) during JJA and considerably increasing it during DJF (Fig. 1~~5~~6).

The close linear correlation ~~relationship~~ identified between lapse rate magnitude and SIE indicates that SIE is an important factor for the development of these variations, especially between May and September.

The phenomenon previously described is likely linked to the development of an inversion layer in the lower troposphere on the western side of the AP mainly during JJA, which in turn is related to a strong radiative imbalance. During JJA, solar radiation diminishes until it reaches a minimum at the winter solstice. The lack of solar radiation leads to considerable cooling that favors the formation of sea ice and in turn, causes differential cooling between the sea ice surface and the air above it. As the sea ice surface cools faster than the air above it, a near–surface altitudinal pattern of increasing temperature develops where local atmospheric stability prevails. The layer of atmospheric stability extends from sea level up to at least 350 m a.s.l, where it turns into an atmospheric instability regime. Both regimes together favor the decrease of the overall lapse rate, as temperature first increases and then decreases with height. Conversely, no inversion layer is formed during DJF due to the absence of sea ice and hence, atmospheric instability prevails, which is related to high lapse rates (Fig. 15~~4~~b and 15~~4~~c).

The existence of an inversion layer during the months with sea ice coverage might explain the low oscillation of monthly mean temperatures estimated at LCL compared to monthly mean air temperatures at BE (OH). The ~~inverse relation~~negative correlation between SAM index and SIE also seems to play an important role, as SAM positive phases enhance the transport of warm and moist air towards the western side of the AP, thus inhibiting the formation of sea ice. This has a direct impact on the lapse rate as the development of an inversion layer is hindered and therefore air temperatures on LCL are regulated. The interaction between SAM and SIE plays a key role as sea–ice–covered conditions temper the maritime system, favoring continental–like conditions and reducing annual mean air temperature, implying a higher temperature amplitude in BE and OH throughout the year.

The temperature time series estimated from the stable water isotope record ($\delta^{18}O$ and d_{excess}) from LCL firn cores exhibits a periodic (biannual) pattern, which can be linked to a similar periodical behavior observed in SAM index and in SIE. The relatively constant temperatures observed during MAM, JJA and SON in years with a positive SAM phase provide evidence that during these seasons condensation is taking place at similar temperatures. Under such conditions (positive SAM), the low variations in the lapse rate throughout the year, along with the low thermal oscillation in BE (OH) explain the presence of a constant condensation temperature, which does not differ much from air temperature during DJF. Conversely, the stronger annual temperature oscillation observed on LCL during negative SAM phases indicates marked variations in condensation temperature throughout the year.

Finally, the proposed inversion layer model (Fig. 16~~5~~) explains the seasonal variations observed in the $\delta^{18}O$–T relationship of precipitation samples from OH. The distortion of the direct relation between condensation temperature and surface air temperature by an inversion layer makes it necessary to differentiate $\delta^{18}O$–T relationship according to the lapse rate evolution throughout the year. In this context, MAM and SON were identified as transitional periods in the formation of the inversion layer, mainly because of the sea–ice formation and retreat during these seasons. The seasonal adjustment considered to estimate LCL temperatures must be applied, because the sea–ice cover varies inter–annually in its duration and extension, which in turn produces the inter–annually variable inversion layer. The proposed model for the coastal region on the western side of the AP at OH latitude, is consistent with the observations of Yaorong et al. (2003) on KGI (South Shetland Islands), where several inversion layers developed extending beyond 400 m a.s.l.

6 Conclusions

In this study, we examined one of the most complete records of recent precipitation from the northern AP, with a total of 210 single precipitation events and more than 60 m of firn cores. The firn cores retrieved in this work include the accumulation at the northwestern AP region between 2008 and 2014. Precipitation and firn stable water isotope compositions have been compared to different meteorological data sets to determine their representativeness as climate proxies for the region.

The results of our study reveal significant seasonal changes in the $\delta^{18}O$–T relationship throughout the year. For autumn and spring a $\delta^{18}O$–T ratio of 0.69‰ °C^{-1} (R= 0.74) was found to be most representative, whereas for winter and summer the $\delta^{18}O$–T ratio appears to be highly dependent on SIE conditions. The apparent moisture source for air parcels precipitating at the northern AP is mainly located in the Bellingshausen Sea and in the southern Pacific Ocean. The transport of water vapor along these oceanic and coastal pathways exerts a strong impact on the d_{excess} signal of precipitation. The comparison between the d_{excess} signal from the moisture source and the d_{excess} signal from firn cores has been used successfully to date the firn cores from the northern AP, yielding a seven–year isotopic time series in high temporal resolution for LCL.

Based on our dating method we could define LCL as a high snow accumulation site, with a mean annual accumulation rate of 1770 kg m^{-2} y^{-1} for the period 2006–2014. Accumulation is highly variable from year to year, with a maximum and minimum of 2470 kg m^{-2} (in 2008) and 1060 kg m^{-2} (in 2010), respectively. In addition, we identified the presence of a strong orographic precipitation effect along the western side of the AP reflected by an accumulation increase with altitude (1500 kg m^{-2} y^{-1} km^{-1}), as well as by the isotopic depletion of precipitation from sea level up to LCL (-2.40‰ km^{-1} for autumn) and from the coast line up to the ice divide (-0.08 ‰ km^{-1}).

The maritime regime present on the western side of the AP has a strong control on air temperatures, observed as restricted summer/winter oscillation, and is reflected in a poor seasonality of the $\delta^{18}O$ and δD profiles in firn cores. Recent climatic conditions can be only reconstructed from $\delta^{18}O$ time series obtained from LCL firn cores when considering an inversion layer model during winter season. The strength of the inversion layer likely depends on SIE and SAM index values. Taking into account the effect of the inversion layer on the isotope–temperature relationship, we observe a slight cooling trend of mean annual air temperature at LCL with an approximate rate of -0.33°C y^{-1} for the period sampled by the examined firn cores (2009-2014). This finding is in line with evidence from stacked meteorological record of the nearby research stations as determined by Turner et al. (2016).

Our results demonstrate that the stable water isotope composition of firn cores retrieved from LCL is capable of reproducing the meteorological signal present in this region, validating it as a valuable proxy for paleo–climate reconstructions in the northern AP region. Environmental (atmosphere and ocean) and glaciological conditions present at LCL, a ~350 m thick ice cap, together with an almost undisturbed isotopic record are optimal prerequisites for the preservation of a climate proxy record with a high temporal resolution. Consequently, LCL is a suitable site for recovering a medium–depth ice core to investigate climate variations during the last centuries in the northern AP region.

6 Acknowledgements

The present work was funded by the FONDECYT project 11121551 and supported by the Chilean Antarctic Institute (INACH), the Chilean Air Force and Army logistic facilities. We want to show our gratitude to the Universidad Nacional Andres Bello for supporting this study. We also greatly thank our colleagues, who made field work conditions less severe, especially to Daniel Rutllant for his support on the logistic and field safety. We would like to thank all people involved on the laboratory work, especially to Ivonne Quintanilla, who carried out the sample processing at UNAB and to Dr. Johannes Freitag, for his support with the X-Ray tomography processing at AWI. Tracy Wormwood is greatly thanked for her support editing this manuscript. We highly appreciate the comments of two anonymous reviewers, who provided helpful observations that greatly contributed to improve this manuscript. Finally, we thank the dedicated work of the editor of this article Benjamin Smith.

References

Abram, N. J., Mulvaney, R., Wolff, E. W., Triest, J., Kipfstuhl, S., Trusel, L. D., Vimeux, F., Fleet, L., and Arrowsmith, C.: Acceleration of snow melt in an Antarctic Peninsula ice core during the twentieth century, Nature Geosci, 6, 404-411, doi: 10.1038/ngeo1787, 2013.

Aristarain, A., Jouzel, J., and Pourchet, M.: Past Antarctic Peninsula climate (1850-1980) deduced from an ice core istope record, Climatic Change, 9, 69-89, 1986.

Aristarain, A., Jouzel, J., and Lorius, C.: A 400 Year Isotope record of the Antarctic Peninsula climate, Geophys. Res. Lett., 17, 2369-2372, doi: 10.1029/GL017i013p02369, 1990.

Aristarain, A., Delmas, R., and Stievenard, M.: Ice-Core Study of the link between Sea-Salt aerosol, Sea-Ice cover and climate in the Antarctic Peninsula Area, Climatic Change, 67, 63-86, 2004.

Bintanja, R.: The local surface energy balance of the Ecology Glacier, King George Island, Antarctica: measurements and modelling, Antarctic Science, 7, 315-325, doi: 10.1017/S0954102095000435, 1995.

Bromwich, D. H., Nicolas, J. P., Monaghan, A. J., Lazzara, M. A., Keller, L. M., Weidner, G. A., and Wilson, A. B.: Central West Antarctica among the most rapidly warming regions on Earth, Nature Geosci, 6, 139-145, doi: 10.1038/ngeo1671, 2013.

Cárdenas, C., Johnson, E., Fernandoy, F., Meyer, H., Cereceda, F., and Vidal, V.: Preliminary results of the superficial and sub-glacier topography survey using Radio Echo Sounding at the La Claveré Plateau, Antarctic Peninsula, SCAR Open Science Conference, Auckland, New Zealand, 1-3 September, 2014.

Carrasco, J. F.: Decadal Changes in the Near-Surface Air Temperature in the Western Side of the Antarctic Peninsula, Atmospheric and Climate Sciences, 03, 7, doi: 10.4236/acs.2013.33029, 2013.

Clark, I., and Fritz, P.: Environmental Isotopes in Hydrogeology, edited by: Stein, J., and Starkweather, A., Lewis, Boca Raton, New York, 311 pp., 1997.

Craig, H.: Isotopic variations in meteoric waters, Science, 133, 1702-1703, doi: 10.1126/science.133.3465.1702, 1961.

Dalla Rosa, J.: Variabilidade da taxa de acumulação de neve no Platô Detroit, Península Antártica, M.S. thesis, Instituto de Geociências, Universidade Federal do Rio Grande do Sul, Porto Alegre, 98 pp., 2013.

Dierssen, H. M., Smith, R. C., and Vernet, M.: Glacial meltwater dynamics in coastal waters west of the Antarctic peninsula, Proceedings of the National Academy of Sciences, 99, 1790-1795, doi: 10.1073/pnas.032206999, 2002.

Draxler, R. R., and Hess, G. D.: An Overview of the HYSPLIT-4 modelling system for trajectories, dispersion and deposition, Aust. Meterol. Mag., 47, 295-308, 1998.

Dutrieux, P., De Rydt, J., Jenkins, A., Holland, P. R., Ha, H. K., Lee, S. H., Steig, E. J., Ding, Q., Abrahamsen, E. P., and Schröder, M.: Strong Sensitivity of Pine Island Ice-Shelf Melting to Climatic Variability, Science, 343, 174-178, doi: 10.1126/science.1244341, 2014.

Falk, U., and Sala, H.: Winter melt conditions of the inland ice cap on King George Island, Antarctic Peninsula, Erkunde, 69, 341-363, doi: 10.3112/erdkunde.2015.04.04, 2015.

Fernandoy, F., Meyer, H., and Tonelli, M.: Stable water isotopes of precipitation and firn cores from the northern Antarctic Peninsula region as a proxy for climate reconstruction, The Cryosphere, 6, 313-330, doi: 10.5194/tc-6-313-2012, 2012.

Fyfe, J. C., and Saenko, O. A.: Human-Induced Change in the Antarctic Circumpolar Current, Journal of Climate, 18, 3068-3073, doi: 10.1175/JCLI3447.1, 2005.

Fyfe, J. C., Saenko, O. A., Zickfeld, K., Eby, M., and Weaver, A. J.: The Role of Poleward-Intensifying Winds on Southern Ocean Warming, Journal of Climate, 20, 5391-5400, doi: 10.1175/2007JCLI1764.1, 2007.

Gille, S. T.: Decadal-Scale Temperature Trends in the Southern Hemisphere Ocean, Journal of Climate, 21, 4749-4765, doi: 10.1175/2008JCLI2131.1, 2008.

Goodwin, B. P.: Recent Environmental Changes on the Antarctic Peninsula as Recorded in an ice core from the Bruce Plateau, Ph.D. thesis, Graduate Program in Atmospheric Science, Ohio State University, 247 pp., 2013.

Goodwin, B. P., Mosley-Thompson, E., Wilson, A. B., Porter, S. E., and Sierra-Hernandez, M. R.: Accumulation Variability in the Antarctic Peninsula: The Role of Large-Scale Atmospheric Oscillations and Their Interactions, Journal of Climate, 29, 2579-2596, doi: 10.1175/JCLI-D-15-0354.1, 2015.

Harig, C., and Simons, F. J.: Accelerated West Antarctic ice mass loss continues to outpace East Antarctic gains, Earth and Planetary Science Letters, 415, 134-141, doi: 10.1016/j.epsl.2015.01.029, 2015.

Jiahong, W., Jiancheng, K., Jiankang, H., Zichu, X., Leibao, L., and Dali, W.: Glaciological studies on the King George Island ice cap, South Shetland Islands, Antarctica, Annals of Glaciology, 27, 105-109, doi: 10.3198/1998AoG27-1-105-109, 1998.

Jiankang, H., Jiancheng, K., Jiahong, W., Lluberas, A., and Rodriguez, F.: General characteristics in stratigraphy and density variation for ice cores from Collins Ice Cap, King George Island, Antarctica, Antarctic Research, 6, 40-46, 1994.

Jouzel, J., Delaygue, G., Landais, A., Masson-Delmotte, V., Risi, C., and Vimeux, F.: Water isotopes as tools to document oceanic sources of precipitation, Water Resources Research, 49, 7469-7486, doi: 10.1002/2013WR013508, 2013.

Kanamitsu, M.: Description of the NMC Global Data Assimilation and Forecast System, Weath. Forecast., 4, 335-342, doi: 10.1175/1520-0434(1989)004<0335:DOTNGD>2.0.CO;2, 1989.

Kennedy, J. J., Rayner, N. A., Smith, R. O., Parker, D. E., and Saunby, M.: Reassessing biases and other uncertainties in sea surface temperature observations measured in situ since 1850: 1. Measurement and sampling uncertainties, Journal of Geophysical Research: Atmospheres, 116, n/a-n/a, 10.1029/2010JD015218, 2011a.

Kennedy, J. J., Rayner, N. A., Smith, R. O., Parker, D. E., and Saunby, M.: Reassessing biases and other uncertainties in sea surface temperature observations measured in situ since 1850: 2. Biases and homogenization, Journal of Geophysical Research: Atmospheres, 116, n/a-n/a, 10.1029/2010JD015220, 2011b.

Kuipers Munneke, P., Picard, G., van den Broeke, M. R., Lenaerts, J. T. M., and van Meijgaard, E.: Insignificant change in Antarctic snowmelt volume since 1979, Geophysical Research Letters, 39, doi: 10.1029/2011GL050207, 2012.

Legrand, M., and Mayewski, P.: Glaciochemistry of polar ice cores: A review, Rev. Geophys., 35, 219-243, doi: 10.1029/96RG03527, 1997.

Linow, S., Hörhold, M. W., and Freitag, J.: Grain-size evolution of polar firn: a new empirical grain growth parameterization based on X-ray microcomputer tomography measurements, Journal of Glaciology, 58, 1245-1252, doi: 10.3189/2012JoG11J256, 2012.

Marshall, G. J.: Trends in the Southern Annular Mode from observations and Reanalyses, J. Climate, 16, 4134-4143, doi: 10.1175/1520-0442(2003)016<4134:TITSAM>2.0.CO;2, 2003.

Marshall, G. J., Orr, A., van Lipzig, N. P. M., and King, J. C.: The Impact of a Changing Southern Hemisphere Annular Mode on Antarctic Peninsula Summer Temperatures, J. Climate, 19, 5388-5404, doi: 10.1175%2FJCLI3844.1, 2006.

Marshall, G. J.: Half-century seasonal relationships between the Southern Annular Mode and Antarctic temperatures, Int. J. Climatol., 27, 373-383, doi: 10.1002/Joc.1407, 2007.

Martin, P. J., and Peel, D. A.: The Spatial Distribution of 10 m Temperatures in the Antarctic Peninsula, Journal of Glaciology, 20, 311-317, doi: 10.3198/1978JoG20-83-311-317, 1978.

Masson-Delmotte, V., Hou, S., Ekaykin, A., Jouzel, J., Aristarain, A., Bernardo, R. T., Bromwich, D., Cattani, O., Delmotte, M., Falourd, S., Frezzotti, M., Gallée, H., Genoni, L., Isaksson, E., Landais, A., Helsen, M. M., Hoffmann, G., Lopez, J., Morgan, V., Motoyama, H., Noone, D., Oerter, H., Petit, J. R., Royer, A., Uemura, R., Schmidt, G. A., Schlosser, E., Simoes, J. C., Steig, E. J., Stenni, B., Stievenard, M., van den Broeke, M. R., van de Wal, R. S. W., van de Berg, W. J., Vimeux, F., and White, J. W. C.: A Review of Antarctic Surface Snow Isotopic Composition: Observations, Atmospheric Circulation, and Isotopic Modeling, J. Climate, 21, 3359-3387, doi: 10.1175%2F2007JCLI2139.1, 2008.

Meredith, M., and King, J. C.: Rapid climate change in the ocean west of the Antarctic Peninsula during the second half of the 20th century, Geophys. Res. Lett., 32, 1 - 5, doi: 10.1029/2005GL024042, 2005.

Meredith, M. P., Stammerjohn, S. E., Venables, H. J., Ducklow, H. W., Martinson, D. G., Iannuzzi, R. A., Leng, M. J., van Wessem, J. M., Reijmer, C. H., and Barrand, N. E.: Changing distributions of sea ice melt and meteoric water west of the Antarctic Peninsula, Deep Sea Research Part II: Topical Studies in Oceanography, doi: 10.1016/j.dsr2.2016.04.019, 2016.

Meyer, H., Schönicke, L., Wand, U., Hubberten, H. W., and Friedrichsen, H.: Isotope Studies of Hydrogen and Oxygen in Ground Ice - Experiences with the Equilibration Technique, Isot. Enviro. Healt. S., 36, 133 - 149, doi: 10.1080/10256010008032939, 2000.

Moser, H., and Stichler, W.: Environmental isotopes in ice and snow, in: Handbook of environmental isotope geochemistry, edited by: Fritz, P., and Fontes, J. C., Elsevier, New York, 141-178, 1980.

Orr, A., Marshall, G. J., Hunt, J. C. R., Sommeria, J., Wang, C.-G., van Lipzig, N. P. M., Cresswell, D., and King, J. C.: Characteristics of Summer Airflow over the Antarctic Peninsula in Response to Recent Strengthening of Westerly Circumpolar Winds, Journal of the Atmospheric Sciences, 65, 1396-1413, 10.1175/2007JAS2498.1, 2008.

Peel, D. A., Mulvaney, R., and Davison, B. M.: Stable-Isotope/Air-Temperature relationship in ice cores from Dolleman Island and the Palmer Land Plateau, Antarctic Peninsula, Ann. Glaciol., 10, 130-136, doi: 10.3198/1988AoG10-130-136, 1988.

Petit, J. R., White, J. W. C., Young, N. W., Jouzel, J., and Korotkevich, Y. S.: Deuterium Excess in Recent Antarctic Snow, J. Geophys. Res-Atmos., 96, 5113-5122, doi: 10.1029/90JD02232, 1991.

Potocki, M., Mayewski, P. A., Kurbatov, A. V., Simões, J. C., Dixon, D. A., Goodwin, I., Carleton, A. M., Handley, M. J., Jaña, R., and Korotkikh, E. V.: Recent increase in Antarctic Peninsula ice core uranium concentrations, Atmospheric Environment, 140, 381-385, http://dx.doi.org/10.1016/j.atmosenv.2016.06.010, 2016.

Pritchard, H. D., and Vaughan, D. G.: Widespread acceleration of tidewater glaciers on the Antarctic Peninsula, J. Geophys. Res., 112, F03S29, doi: 10.1029/2006jf000597, 2007.

Pritchard, H. D., Ligtenberg, S. R. M., Fricker, H. A., Vaughan, D. G., van den Broeke, M. R., and Padman, L.: Antarctic ice-sheet loss driven by basal melting of ice shelves, Nature, 484, 502-505, doi: 10.1038/nature10968, 2012.

Rignot, E., Casassa, G., Gogineni, S., Kanagaratnam, P., Krabill, W., Pritchard, H., Rivera, A., Thomas, R., Turner, J., and Vaughan, D.: Recent ice loss from the Fleming and other glaciers, Wordie Bay, West Antarctic Peninsula, Geophys. Res. Lett., 32, L07502, doi: 10.1029/2004GL021947, 2005.

Rozanski, K., Araguás-Araguás, L., and Gonfiantini, R.: Isotopic Patterns in Modern Global Precipitation, in: Climate Change in Continental Isotopic Records, edited by: Swart, P. K., Lohman, K. C., McKenzie, J., and Savin, S., American Geophysical Union, Washington, USA, 1993.

Rückamp, M., Blindow, N., Suckro, S., Braun, M., and Humbert, A.: Dynamics of the ice cap on King George Island, Antarctica: field measurements and numerical simulations, Ann. Glaciol., 51, 80-90, 2010.

Saigne, C., and Legrand, M.: Measurements of methanesulphonic acid in Antarctic ice, Nature, 330, 240-242, doi: 10.1038/330240a0, 1987.

Seehaus, T., Marinsek, S., Helm, V., Skvarca, P., and Braun, M.: Changes in ice dynamics, elevation and mass discharge of Dinsmoor–Bombardier–Edgeworth glacier system, Antarctic Peninsula, Earth and Planetary Science Letters, 427, 125-135, doi: 10.1016/j.epsl.2015.06.047, 2015.

Shepherd, A., Ivins, E. R., A, G., Barletta, V. R., Bentley, M. J., Bettadpur, S., Briggs, K. H., Bromwich, D. H., Forsberg, R., Galin, N., Horwath, M., Jacobs, S., Joughin, I., King, M. A., Lenaerts, J. T. M., Li, J., Ligtenberg, S. R. M., Luckman, A., Luthcke, S. B., McMillan, M., Meister, R., Milne, G., Mouginot, J., Muir, A., Nicolas, J. P., Paden, J., Payne, A. J., Pritchard, H., Rignot, E., Rott, H., Sørensen, L. S., Scambos, T. A., Scheuchl, B., Schrama, E. J. O., Smith, B., Sundal, A. V., van Angelen, J. H., van de Berg, W. J., van den Broeke, M. R., Vaughan, D. G., Velicogna, I., Wahr, J., Whitehouse, P. L., Wingham, D. J., Yi, D., Young, D., and Zwally, H. J.: A Reconciled Estimate of Ice-Sheet Mass Balance, Science, 338, 1183-1189, doi: 10.1126/science.1228102, 2012.

Sigmond, M., Reader, M. C., Fyfe, J. C., and Gillett, N. P.: Drivers of past and future Southern Ocean change: Stratospheric ozone versus greenhouse gas impacts, Geophysical Research Letters, 38, doi: 10.1029/2011GL047120, 2011.

Simões, J., Ferron, F., Bernardo, R., Aristarain, A., Stievenard, M., Pourchet, M., and Delmas, R.: Ice core study from the King George Island, South Shetlands, Antarctica., Pesquisa Antártica Brasileira, 4, 9-23, 2004.

Sinclair, K. E., Bertler, N. A. N., Trompetter, W. J., and Baisden, W. T.: Seasonality of Airmass Pathways to Coastal Antarctica: Ramifications for Interpreting High-Resolution Ice Core Records, Journal of Climate, 26, 2065-2076, doi: 10.1175/JCLI-D-12-00167.1, 2012.

Stichler, W., Schotterer, U., Fröhlich, K., Ginot, P., Kull, C., Gäggeler, H., and Pouyaud, B.: Influence of sublimation on stable isotope records recovered from high-altitude glaciers in the tropical Andes, J. Geophys. Res., 106, doi: 10.1029/2001jd900179, 2001.

Thomas, E. R., Marshall, G. J., and McConnell, J. R.: A doubling in snow accumulation in the western Antarctic Peninsula, Geophys. Res. Lett., 35, 1-5, doi: 10.1029/2007GL032529, 2008.

Thomas, E. R., and Bracegirdle, T. J.: Improving ice core interpretation using in situ and reanalysis data, J. Geophys. Res., 114, D20116, doi: 10.1029/2009jd012263, 2009.

Thomas, E. R., Dennis, P. F., Bracegirdle, T. J., and Franzke, C.: Ice core evidence for significant 100-year regional warming on the Antarctic Peninsula, Geophys. Res. Lett., 36, -, doi: 10.1029/2009gl040104, 2009.

Thomas, E. R., and Bracegirdle, T. J.: Precipitation pathways for five new ice core sites in Ellsworth Land, West Antarctica, Climate Dynamics, 44, 2067-2078, doi: 10.1007/s00382-014-2213-6, 2015.

Thompson, D. W. J., and Solomon, S.: Interpretation of Recent Southern Hemisphere Climate Change, Science, 296, 895-899, 10.1126/science.1069270, 2002.

Travassos, J., and Simoes, J.: High-resolution radar mapping of internal layers of a subpolar ice cap, King George Island, Antarctica, Pesquisa Antártica Brasileira, 4, 57-65, 2004.

Trusel, L. D., Frey, K. E., and Das, S. B.: Antarctic surface melting dynamics: Enhanced perspectives from radar scatterometer data, Journal of Geophysical Research: Earth Surface, 117, doi: 10.1029/2011JF002126, 2012.

Trusel, L. D., Frey, K. E., Das, S. B., Karnauskas, K. B., Kuipers Munneke, P., van Meijgaard, E., and van den Broeke, M. R.: Divergent trajectories of Antarctic surface melt under two twenty-first-century climate scenarios, Nature Geosci, 8, 927-932, 10.1038/ngeo2563 http://www.nature.com/ngeo/journal/v8/n12/abs/ngeo2563.html#supplementary-information, 2015.

Turner, J., Colwell, S. R., Marshall, G. J., Lachlan-Cope, T. A., Carleton, A. M., Jones, P. D., Lagun, V., Reid, P. A., and Iagovkina, S.: The SCAR READER project: Toward a high-quality database of mean Antarctic meteorological observations, J. Climate, 17, 2890-2898, doi: 10.1175/1520-0442(2004)017<2890:TSRPTA>2.0.CO;2, 2004.

Turner, J., Colwell, S. R., Marshall, G. J., Lachlan-Cope, T. A., Carleton, A. M., Jones, P. D., Lagun, V., Reid, P. A., and Iagovkina, S.: Antarctic climate change during the last 50 years, Int. J. Climatol., 25, 279-294, doi: 10.1002/joc.1130, 2005.

Turner, J., Bindschadler, R. A., Convey, P., Di Prisco, G., Fahrbach, E., Gutt, J., Hodgson, D. A., Mayewski, P. A., and Summerhayes, C. P.: Antarctic Climate Change and the Environment, Scott Polar Research Institute, Scientific Committee on Antarctic Research, Cambridge, UK, 2009.

Turner, J., Lu, H., White, I., King, J. C., Phillips, T., Hosking, J. S., Bracegirdle, T. J., Marshall, G. J., Mulvaney, R., and Deb, P.: Absence of 21st century warming on Antarctic Peninsula consistent with natural variability, Nature, 535, 411-415, doi: 10.1038/nature18645, 2016.

Uemura, R., Matsui, Y., Yoshimura, K., Motoyama, H., and Yoshida, N.: Evidence of deuterium excess in water vapor as an indicator of ocean surface conditions, J. Geophys. Res., 113, 1-10, doi: 10.1029/2008JD010209, 2008.

van Lipzig, N. P. M., Marshall, G. J., Orr, A., and King, J. C.: The Relationship between the Southern Hemisphere Annular Mode and Antarctic Peninsula Summer Temperatures: Analysis of a High-Resolution Model Climatology, Journal of Climate, 21, 1649-1668, 10.1175/2007JCLI1695.1, 2008.

van Wessem, J. M., Reijmer, C. H., van de Berg, W. J., van den Broeke, M. R., Cook, A. J., van Ulft, L. H., and van Meijgaard, E.: Temperature and Wind Climate of the Antarctic Peninsula as Simulated by a High-Resolution Regional Atmospheric Climate Model, Journal of Climate, 28, 7306-7326, doi: 10.1175/JCLI-D-15-0060.1, 2015.

Yaorong, H., Zhenhe, X., and Cong, X.: A Study on Snowstorm Weather in Coastal Area of Western Antarctic, Marine Science Bulletin, 5, 24-31, 2003.

Zagorodnov, V., Nagornov, O., Scambos, T. A., Muto, A., Mosley-Thompson, E., Pettit, E. C., and Tyuflin, S.: Borehole temperatures reveal details of 20th century warming at Bruce Plateau, Antarctic Peninsula, The Cryosphere, 6, 675-686, 10.5194/tc-6-675-2012, 2012.

Zamoruyev, V. V.: Results of glaciological observations at Bellingshausen station in 1968, Trudy Sovetskoy Antarkticheskoy Ekspeditsii, 55, 135-144, 1972.

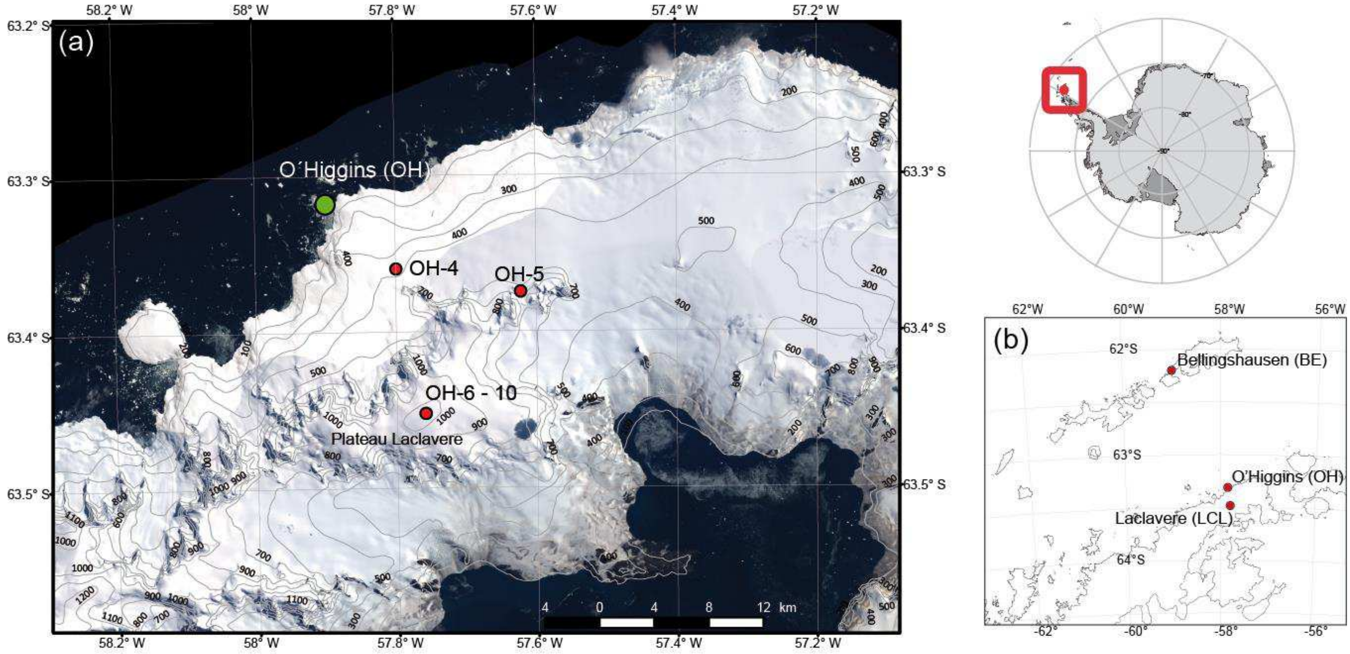

Figure 1: Study area and location of the firn cores presented in this work. (a) Detail of the study zone: the green point shows the Chilean Station O’Higgins (OH) at the west coast of the Antarctic Peninsula. Firn cores retrieved between 2008 and 2015 are shown by red dots. (b) Location of O’Higgins and Bellingshausen Station and Laclavere Plateau, which are mentioned through the text. Satellite image (Landsat ETM+) and digital elevation model (RADARSAT) available from the Landsat Image Mosaic of Antarctica (LIMA) (http://lima.usgs.gov/).

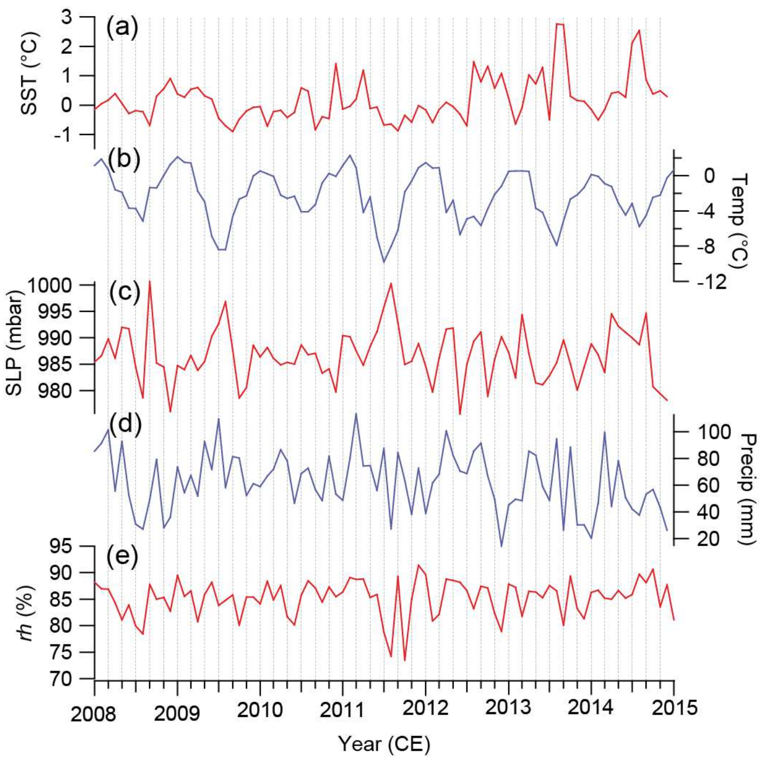

Figure 2: Monthly meteorological ~~monthly~~ data sets used in this study~~,~~ (a) Sea surface temperature (SST), (b) Air temperature (Temp), (c) Sea level pressure (SLP) and (d) Precipitation amount (Precip) from Bellingshausen Station (BE) on King George Island and (e) Relative humidity (*rh*) from the Southern Ocean surrounding the northern Antarctic Peninsula (AP) region. Data shown in the figure is available from the READER dataset (https://legacy.bas.ac.uk/met/READER/) (Turner et al., 2004).

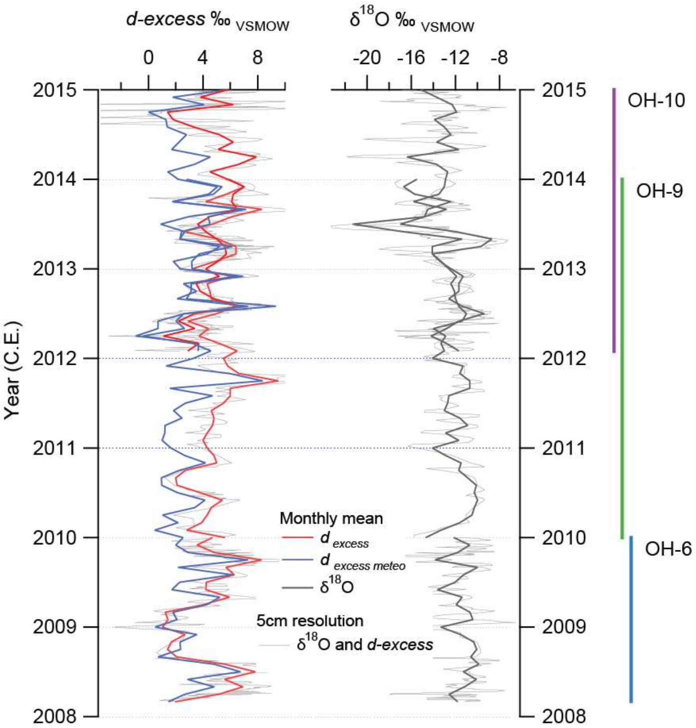

Figure 3: Time series for firn cores OH-6 (light blue line right), OH-9 (green light right) and OH-10 (purple line right) derived for $\delta^{18}O$ (black line right) and d_{excess} (red line left) records using a theoretical d_{excess} ($d_{excess\ meteo}$) value (blue line left). The $d_{excess\ meteo}$ is calculated from- Sea ~~surface~~ Surface ~~temperature~~ Temperature (SST) and Relative Humidity (*rh*) according to Uemura et al. (2008). All three cores are located at the same location within the GPS navigator horizontal error (<10m).

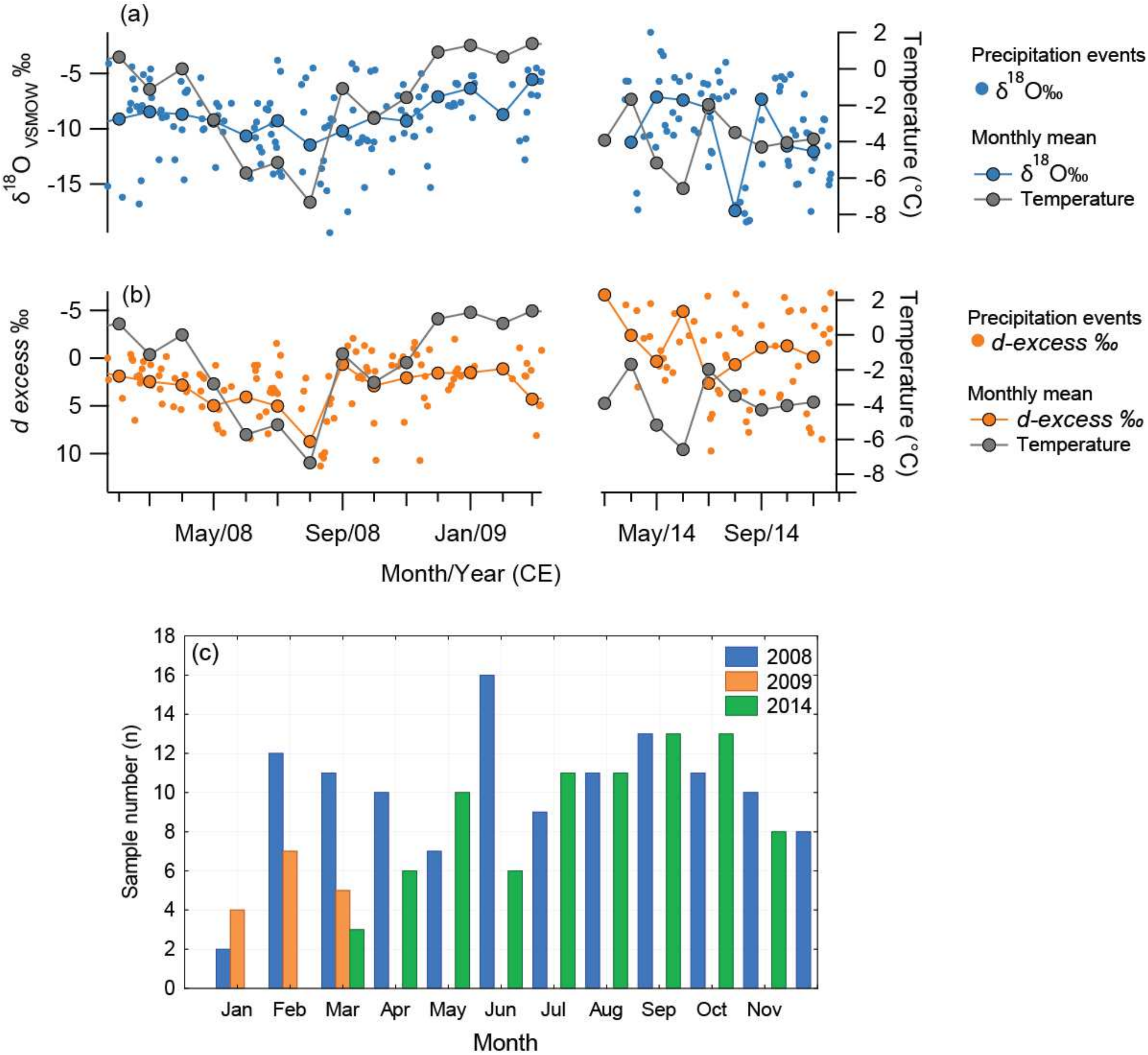

Figure 4: Stable water isotope composition of precipitation events and air temperature at O'Higgins Station. (a) shows the $\delta^{18}O$ composition of precipitation of single daily events (small solid blue dots) and monthly means (big solid blue dots and line) and (b) deuterium excess (d_{excess}) of single daily events (small orange dots) and monthly means (big orange dots and line). In both (a) and (b) monthly mean air temperature is also shown (grey solid dots and line). (c) Histogram showing the monthly distribution of precipitation samples (n) collected at O'Higgins Station in 2008, 2009 and 2014

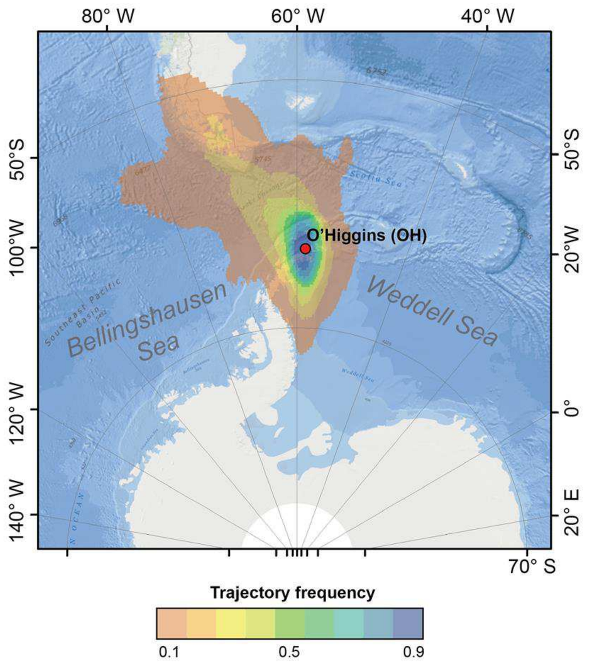

Figure 5: Frequency distribution map of the main transport paths of air masses approaching the northern Antarctic Peninsula (AP). Translucent red colours represent the lowest frequency and blue colours the higher frequency. In general most of the air masses arriving at the AP are coming from the Bellingshausen Sea and the South Pacific Ocean.

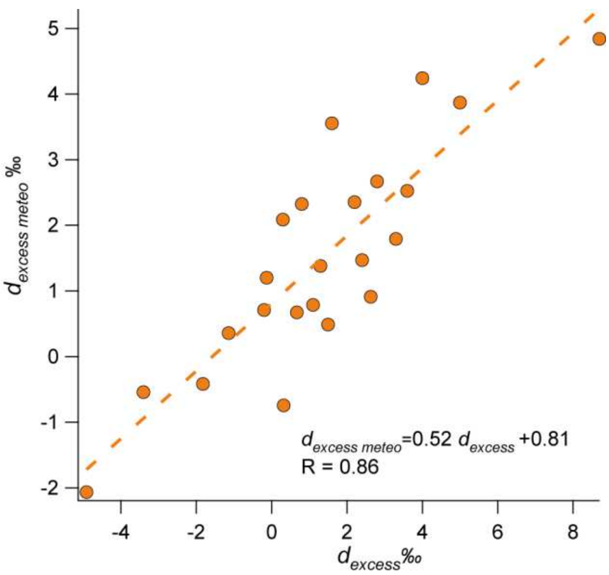

Figure 6: Correlation between monthly mean deuterium excess values (d_{excess}) from precipitation samples and theoretical deuterium excess values calculated from meteorological parameters of the moisture source region ($d_{excess\ meteo}$) according to Uemura et al. (2008).

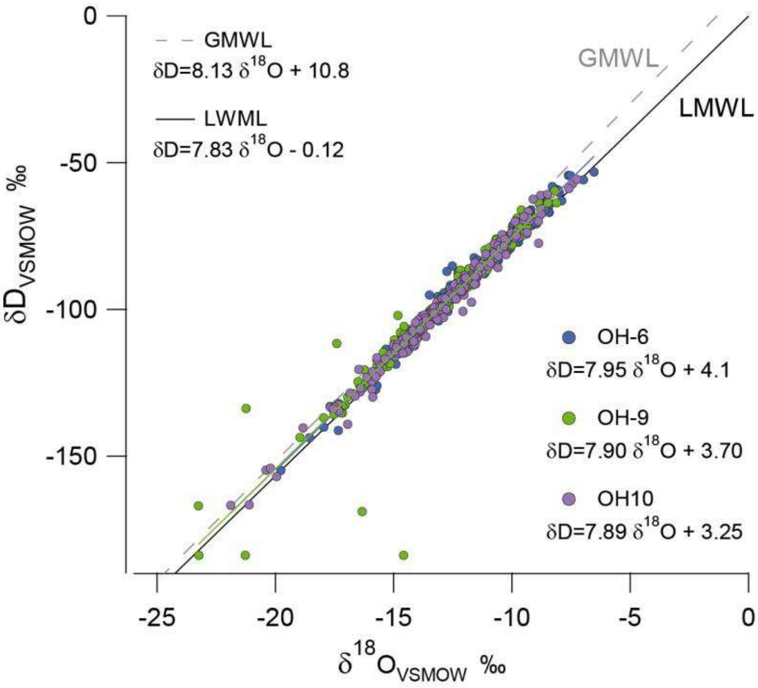

Figure 7: Co-isotopic regression ~~lationship~~ of firn cores OH-6 (solid blue dots), OH-9 (solid green dots) and OH-10 (solid purple dots). All slopes and intercepts are very close to each other as well as to the global and local meteoric water line (GMWL – grey dashed line, and LMWL –black solid line, ~~respecitvely~~respectively). Stable water isotope analysis for each firn core was made at 5 cm resolution, representing 630 samples in total.

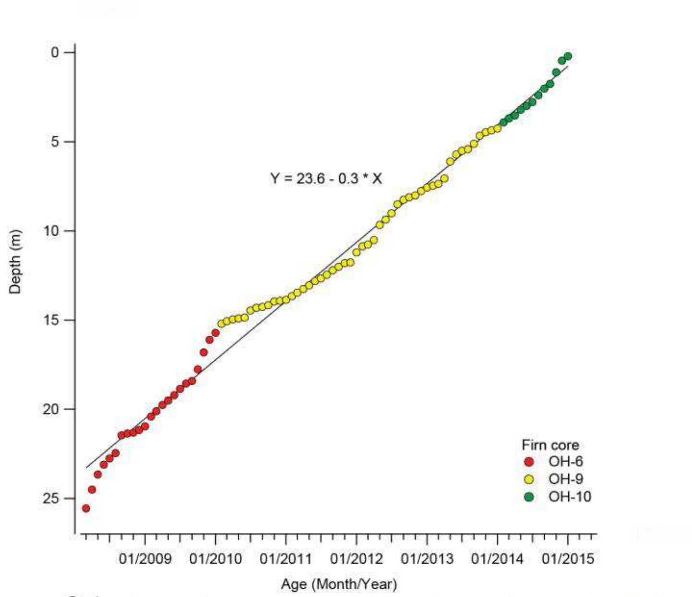

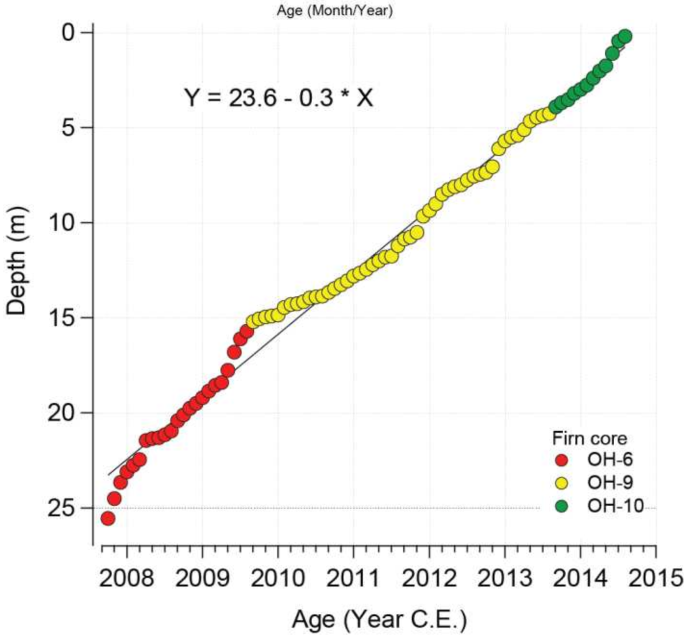

Figure 8: Depth–Age model for firn cores OH-6, OH-9 and OH-10 retrieved from Laclavere Plateau. The linear relationship between depth and time was constructed based on the cores measured d_{excess} oscillation and a synthetically constructed d_{excess} from meteorological observations. Note that the Depth axis was intentionally inverted to visualize the surface (0 m) on top.

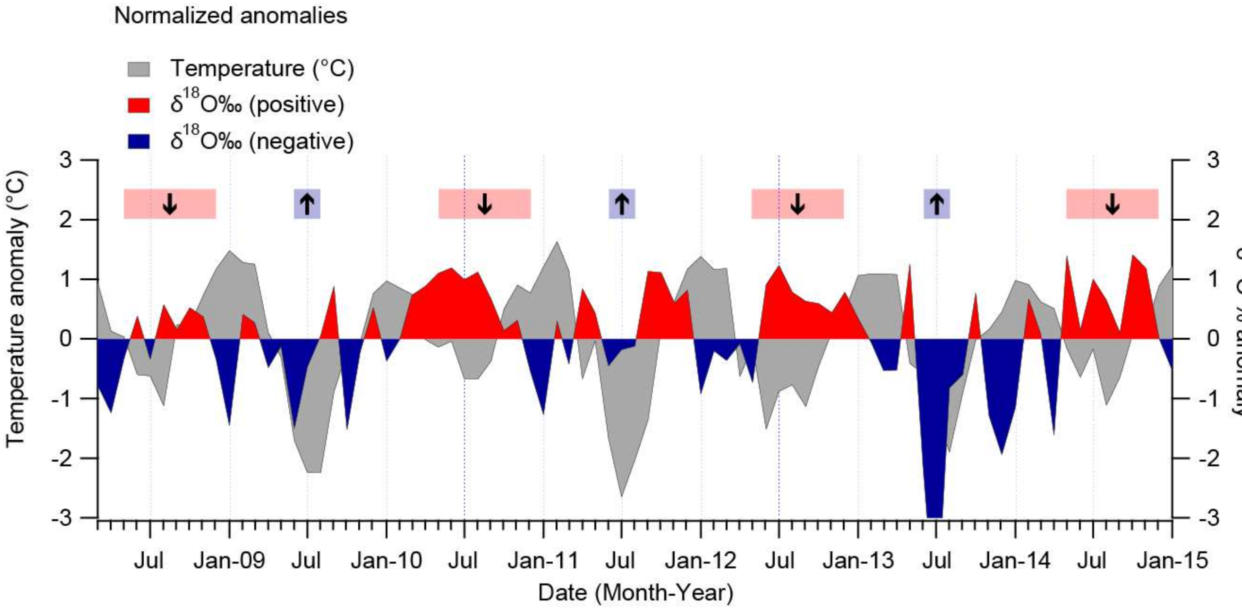

Figure 9: ~~Standarized~~Standardized anomalies for air (monthly mean) temperatures (solid grey colours) registered at Bellingshausen Station (BE) on King George Island and a composite δ^{18}O time series derived from firn cores OH-6, OH-9 and OH-10 from Laclavere Plateau (LCL). Upper transluc<u>ent</u>~~id~~ red (blue) boxes show period of positive (negative) anomalies, down (up) arrow shows the ~~inverse~~ <u>negative</u> (positive) stable water isotope – temperature relationship. Both time series were detrended prior to constructing the time series of anomalies.

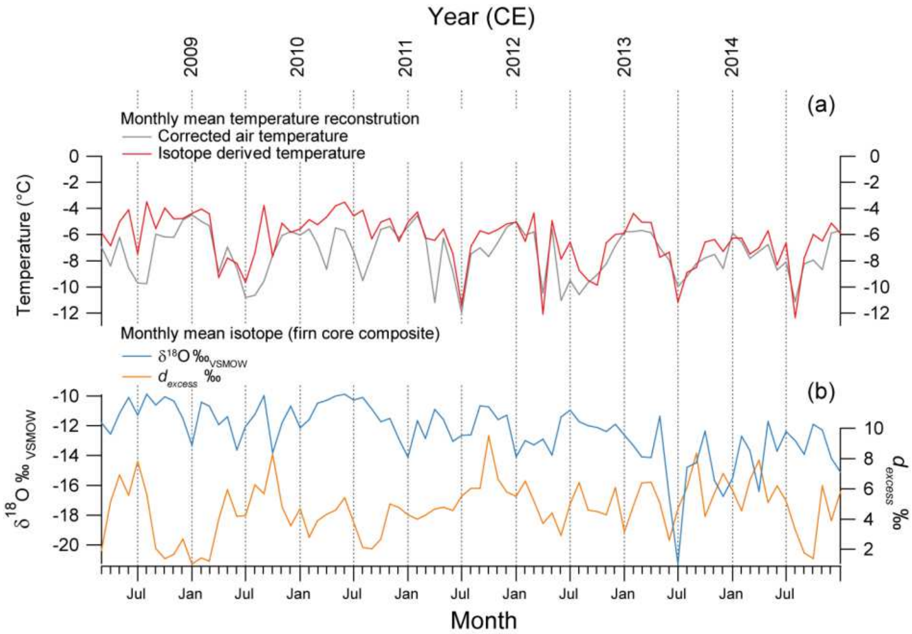

Figure 10: (a) Monthly mean air temperature reconstruction for LCL between March 2008 and January 2015 based on air temperature corrected by a seasonal factor and altitudinal gradient (grey line) and based on a δ^{18}O composite time series derived from firn cores from LCL corrected by a seasonal factor (red line), respectively. (b) δ^{18}O and d_{excess} monthly mean composite time series of LCL firn cores used for the temperature reconstruction of the upper panel.

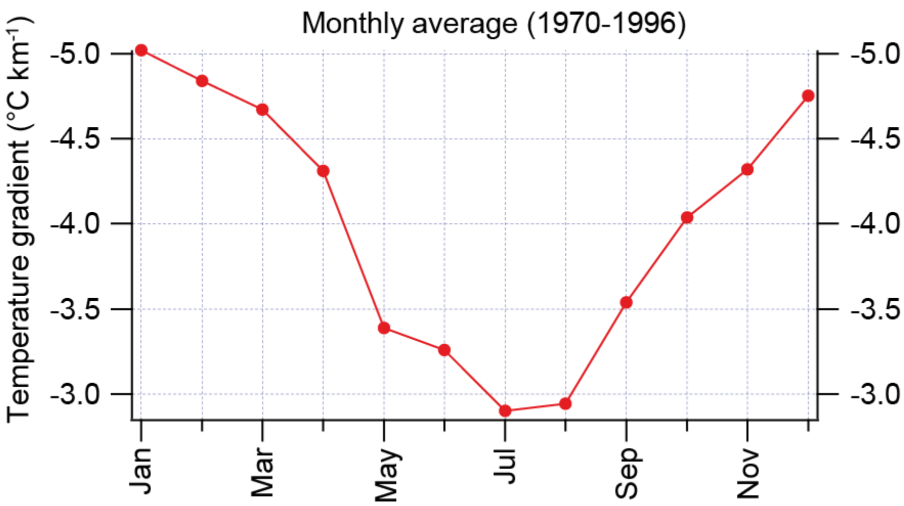

Figure 11: Temperature lapse rate from sea level to 850 hPa level at Bellingshausen station (BE), King George Island, Antarctica. The data is shown as the monthly mean value of observation between 1979 and 1996 (SCAR Reference Antarctic Data for Environmental Research).

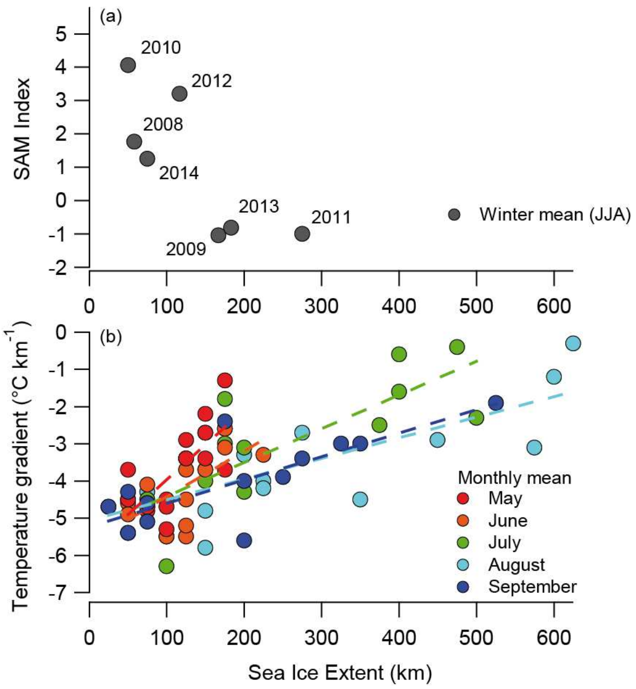

Figure 12: Sea ice extent (SIE) from O'Higgins Station (OH) and its relationship to (a) the Southern Annular Mode and (b) to the temperature gradient between sea level and 1100 m a.s.l. at the Laclavere Plateau (LCL). SIE data is from the National Snow & Ice Data Center data set (NSIDC). Sea ice extent, defined as the extens~~t~~ion of the ~~sea~~ oceanic region covered ~~for~~ by at least 15% ~~of~~ ice, exhibits a negative relationship to the Southern Annular Mode between 2008 and 2014. The relationship to the temperature gradient is positive. A decreasing seasonal pattern of the temperature gradient can be observed from May to September (1979 – 1996).

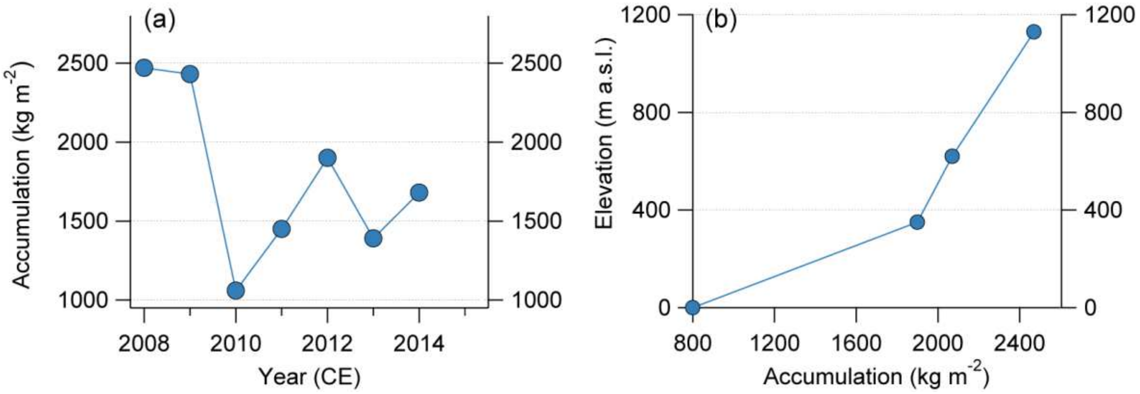

Figure 13: (a) Accumulation rates for Plateau Laclavere during 2008 – 2014 estimated from the stable water isotope composition of firn cores OH-6, OH-9 and OH-10 and their respective density profiles. (b) Accumulation variability for the west flank of the northern Antarctic Peninsula from the coast to Laclavere Plateau. Accumulation rates were derived from precipitation at O'Higgins Station at sea level and firn cores (OH-4, OH-5 and OH-6) for higher altitudes.

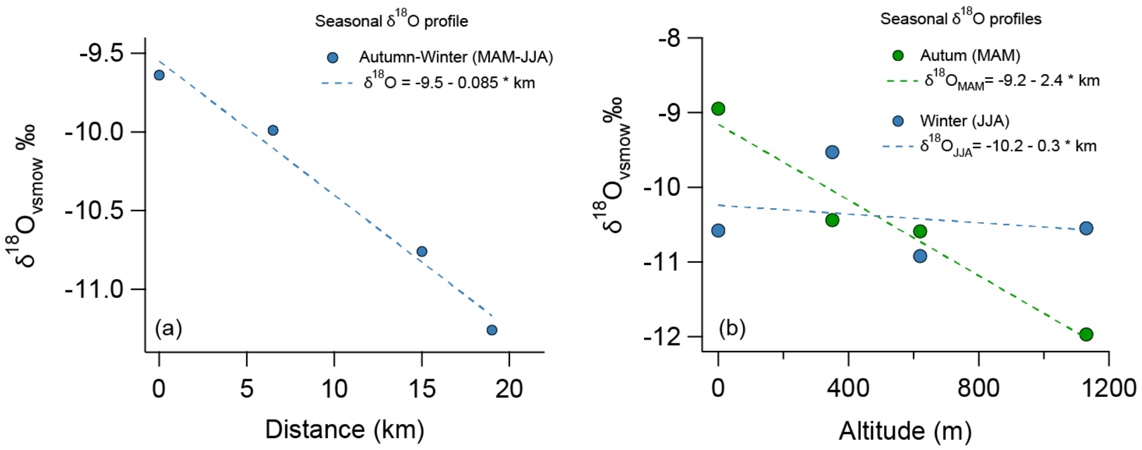

Figure 14: $\delta^{18}O$ profile with relation to (a) the distance from the coast at O'Higgins Station (OH) and at different points on the west flank of the AP (6.5 km (OH-4), 15 km (OH-5) and 19 km (OH-6)) and (b) altitude at 350 m (OH-4), 620 m (OH-5) and 1130 m a.s.l. (OH-6) during autumn (MAM) (green solid dots) and winter (JJA) (blue solid dots).

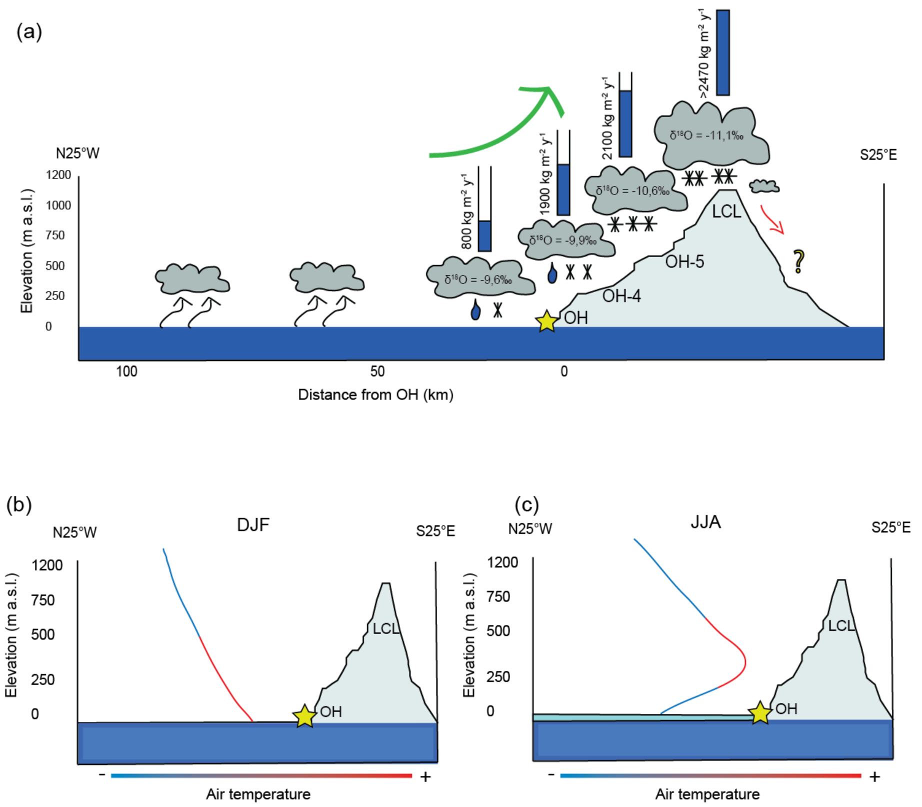

Figure 15: (a) Schematic chart showing the orographic barrier effect of the AP on the stable water isotope depletion and accumulation rate at different altitudes, firn core locations (OH-4, OH-5 and OH-6) and distances from the coast (OH); (b) temperature gradient (adiabatic cooling) during DJF (summer) and sea–ice–free conditions; (c) inversion layer in the lower troposhere during sea–ice–covered conditions in JJA (winter).

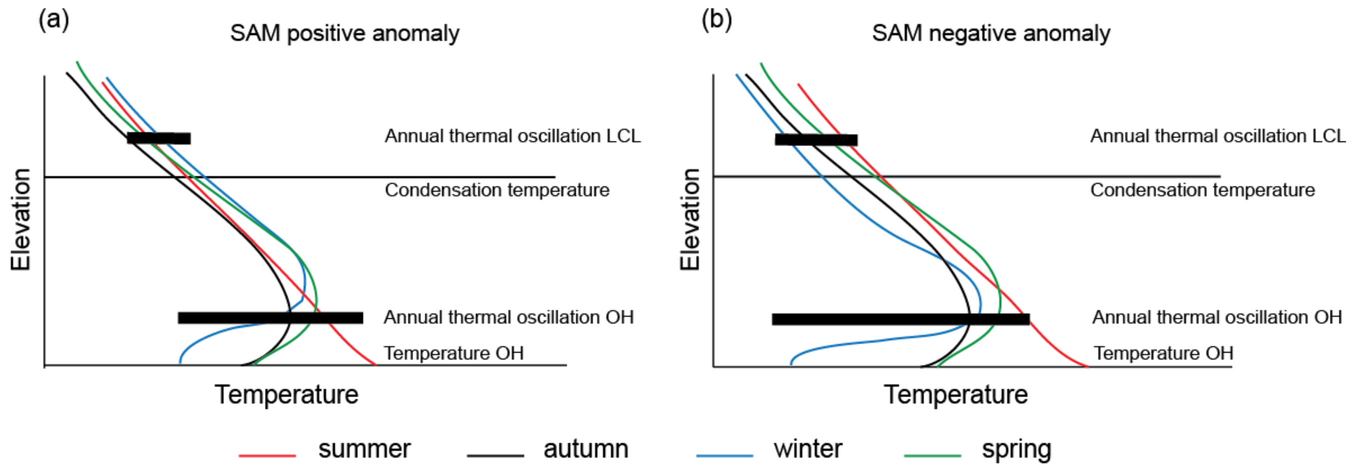

Figure 16: Sea level to LCL temperature oscillation scheme during summer (DJF), autumn (MAM), winter (JJA) and spring- under: (a) positive SAM anomaly conditions and (b) negative SAM anomaly conditions.

Table 1: Statistical summary of the geographical location and water stable isotope composition of all firn cores examined in this work. OH-4 and OH-5 correspond to cores retrieved on the west side of the AP, whereas OH-6, OH-9 and OH-10 were retrieved at LCL on the east–west divide. All cores were analyzed in a 5 cm resolution.

Core	OH-4	OH-5	OH-6	OH-9	OH-10
Coordinates	57.80°W, 63.36°S	57.62°W, 63.38°S	57.76°W, 63.45°S	57.76°W, 63.45°S	57.76°W, 63.45°S
Altitude (m a.s.l.)	350	620	1130	1130	1130
Depth (m)	15.8	10.6	11.0	11.7	10.2
Drilling date	Jan 2009	Jan 2009	Jan 2010	Jan 2014	Jan 2015
$\delta^{18}O$ (‰)					
Mean	-10.4	-10.2	-12.0	-12.8	-12.9
Sdev	1.2	1.5	2.5	2.5	2.6
Min	-14.1	-14.2	-19.8	-23.3	-21.9
Max	-7.0	-7.2	-6.5	-8.1	-7.3
δD (‰)					
Mean	-78.9	-78.1	-91.4	-97.5	-98.8
Sdev	9.7	12.0	19.4	21.0	20.5
Min	-108.2	-111.2	-154.9	-183.8	-166.8
Max	-54.0	-52.1	-53.2	-59.6	-55.8
d_{excess} (‰)					
Mean	4.0	3.9	4.4	5.1	4.7
Sdev	1.5	1.7	2.8	1.9	2.7
Min	0.5	-0.6	-2.6	0.0	-6.5
Max	8.6	8.2	15.0	11.0	11.3
n (samples)	318	213	208	232	190

Table 2: Statistics of the stable water isotope composition of precipitation samples collected at OH Station on the AP 2008–2009 and 2014.

Station	O'Higgins	O'Higgins
Sampling interval	Feb 2008 – Mar 2009	Apr – Nov 2014
Coordinates	63.32°S, 57.90°W	63.32°S, 57.90°W

$\delta^{18}O$ (‰)		
Mean	-9.2	-10.1
Sdev	3.3~~3~~	4.4~~39~~
Min	-19.4	-18.4~~3~~
Max	-3.8	-1.3~~28~~
δD (‰)		
Mean	-70.5	-81.9~~86~~
Sdev	26.44	34.2~~1~~
Min	-150.6	-148.4~~36~~
Max	-21.8	-16.0~~5.99~~
d_{excess} (‰)		
Mean	2.7	3.84
Sdev	4.2~~15~~	4.7~~67~~
Min	-6.6	-1.8~~75~~
Max	22.3	14.7
n (samples)	139	69

Table 3: Statistical correlations and linear regression significance of the $\delta^{18}O$ and d_{excess}–Temperature relationship for precipitation samples. The Slope and Standard error are related to the linear regression constructed from the isotope–Temperature regressions at daily and monthly scales.

	Corr. coef. (R)	Slope (s)	Std. Error	p-value
	Precipitacion $\delta^{18}O_{daily}$–T_{daily}			
DJF	0.81	1.17	0.62	0.01
MAM	0.65	0.77	2.08	<0.01
JJA	0.63	0.35	1.74	0.01
SON	0.6	0.61	2.88	0.03
	Precipitacion $\delta^{18}O_{monthly}$– T_{montly}			
All data–set	0.30	0.28	2.36	>0.05
2008-2009	0.74	0.41	1.03	<0.01
2014	-0.32	-0.77	3.60	>0.05
	Precipitacion d_{excess}–T_{daily}			

DJF	-0.37	-0.86	1.66	>0.1
MAM	0.09	0.10	2.61	>0.1
JJA	-0.28	-0.29	3.61	>0.1
SON	-0.42	-0.74	5.97	>0.1
	Precipitacion d_{excess}–T_{montly}			
All data–set	0.06	0.07	2.98	>0.05
2008–2009	-0.77	-0.60	1.43	<0.01
2014	0.33	0.65	2.35	>0.05

Table 4~~3~~: Correlation between deuterium excess ($d_{excess\ meteo}$) values calculated from monthly mean meteorological data (SST and *rh*) and water stable isotope monthly means for all cores used in this study. Degrees of freedom (df) defined as: n-2 for each correlation.

Core	OH-4	OH-5	OH-6	OH-9	OH-10
Time interval	Jan 2006 – Jan 2009	Mar 2007 – Jan 2009	Mar 2008 – Jan 2010	Feb 2010 – Jan 2014	Feb 2012 – Jan 2015
Corr. coefficient	0.72	0.79	0.81	0.78	0.67
p-value	<0.01	<0.01	<0.01	<0.01	<0.01
df	34	21	21	47	34

Table ~~4~~5: Accumulation rates calculated for all firn cores used in this study. All rates are shown as seasonal and annual mean values with respect to the time interval covered by each core.

	AP Accumulation (kg m^{-2})				
	Western Flank		LCL		
	OH-4	OH-5	OH-6	OH-9	OH-10
DJF-MAM	1121				
JJA-SON	1300				
2006	**2510**				
DJF-MAM	1650	>1380			
JJA-SON	1300	1150			
2007	**2950**	**>2530**			
DJF-MAM	1130	1020	>1530		
JJA-SON	770	1050	940		
2008	**1900**	**2070**	**>2470**		
DJF-MAM			1090		
JJA-SON			1340		
2009			**2430**		
DJF-MAM				700	
JJA-SON				360	
2010				**1060**	
DJF-MAM				680	

JJA-SON	770	
2011	**1450**	
DJF-MAM	1170	1080
JJA-SON	730	690
2012	**1900**	**1770**
DJF-MAM	890	930
JJA-SON	500	690
2013	**1390**	**1620**
DJF-MAM		630
JJA-SON		1050
2014		**1680**